Accepted Manuscript

Magnetic field and nano-scaffolds with stem cells to enhance bone regeneration

Yang Xia, Jianfei Sun, Liang Zhao, Feimin Zhang, Xing-Jie Liang, Yu Guo, Michael D. Weir, Mark A. Reynolds, Ning Gu, Hockin H.K. Xu

PII: S0142-9612(18)30595-7

DOI: 10.1016/j.biomaterials.2018.08.040

Reference: JBMT 18846

To appear in: *Biomaterials*

Received Date: 22 June 2018

Revised Date: 10 August 2018

Accepted Date: 20 August 2018

Please cite this article as: Xia Y, Sun J, Zhao L, Zhang F, Liang X-J, Guo Y, Weir MD, Reynolds MA, Gu N, Xu HHK, Magnetic field and nano-scaffolds with stem cells to enhance bone regeneration, *Biomaterials* (2018), doi: 10.1016/j.biomaterials.2018.08.040.

Magnetic field and nano-scaffolds with stem cells to enhance bone regeneration

Yang Xia[1,2,3], Jianfei Sun[2], Liang Zhao[3,4], Feimin Zhang[1,5], Xing-Jie Liang[6], Yu Guo[1], Michael D. Weir[3], Mark A. Reynolds[3], Ning Gu[2,5], Hockin H. K. Xu[3,7,8]

[1]Jiangsu Key Laboratory of Oral Diseases, Nanjing Medical University, Nanjing, Jiangsu 210029, China;

[2]Jiangsu Key Laboratory for Biomaterials and Devices, School of Biological Science and Medical Engineering, Southeast University, Nanjing, Jiangsu 210096, China;

[3]Department of Advanced Oral Sciences & Therapeutics, University of Maryland School of Dentistry, Baltimore, MD 21201, USA;

[4]Department of Orthopedic Surgery, Nanfang Hospital, Southern Medical University, Guangzhou, Guangdong 510515, China;

[5]Collaborative Innovation Center of Suzhou Nano Science and Technology, Suzhou, Jiangsu 215123, China;

[6]Chinese Academy of Sciences (CAS) Center for Excellence in Nanoscience, CAS Key Laboratory for Biomedical Effects of Nanomaterials and Nanosafety, National Center for Nanoscience and Technology, Beijing 100190, China;

[7]Center for Stem Cell Biology and Regenerative Medicine, University of Maryland School of Medicine, Baltimore, MD 21201, USA;

[8]University of Maryland Marlene and Stewart Greenebaum Cancer Center, University of Maryland School of Medicine, Baltimore, MD 21201, USA

For: *Biomaterials*

(Invited review, submitted in June 2018; revised and resubmitted in August 2018)

Correspondence: Dr. Ning Gu, email: guning@seu.edu.cn.
Dr. Hockin H. K. Xu, email: hxu@umaryland.edu

Short title: Magnetic fields and nano-scaffolds with stem cells to enhance bone regeneration

Key words: Magnetic nanoparticles, scaffolds, stem cells, magnetic forces, osteogenic differentiation, bone regeneration.

Abstract

Novel strategies utilizing magnetic nanoparticles (MNPs) and magnetic fields are being developed to enhance bone tissue engineering efficacy. This article first reviewed cutting-edge research on the osteogenic enhancements via magnetic fields and MNPs. Then the current developments in magnetic strategies to improve the cells, scaffolds and growth factor deliveries were described. The magnetic-cell strategies included cell labeling, targeting, patterning, and gene modifications. MNPs were incorporated to fabricate magnetic composite scaffolds, as well as to construct delivery systems for growth factors, drugs and gene transfections. The novel methods using magnetic nanoparticles and scaffolds with magnetic fields and stem cells increased the osteogenic differentiation, angiogenesis and bone regeneration by 2-3 folds over those of the controls. The mechanisms of magnetic nanoparticles and scaffolds with magnetic fields and stem cells to enhance bone regeneration were identified as involving the activation of signaling pathways including MAPK, integrin, BMP and NF-κB. Potential clinical applications of magnetic nanoparticles and scaffolds with magnetic fields and stem cells include dental, craniofacial and orthopedic treatments with substantially increased bone repair and regeneration efficacy.

1. Introduction

Physical stimulations, including tensile and compressive stresses, fluid shear stresses and heat, are known to be able to significantly enhance bone regeneration and fracture-healing [1,2]. Furthermore, magnetic stimulations from static magnetic fields (SMFs) and electromagnetic fields (EMFs) can also substantially improve bone repair and regeneration

[3,4]. Indeed, magnetic nanoparticles (MNPs) have great potential for bone tissue engineering applications. Used alone, or in combination with a magnetic field, MNPs can help modify and improve the three key factors in bone regeneration: (1) stem cells, (2) scaffolds, and (3) growth factors. Magnetic fields can influence the ion channels and biochemical pathways of the cells. Magnetic-cell strategies include cell labeling, targeting, patterning, and gene modification. Magnetic scaffolds can be prepared with the aid of MNPs and magnetic fields; they can be actuated by a magnetic field to enhance the cells via magneto-mechanical stimulations [5]. In addition, MNPs can serve as delivery systems for growth factors, drugs and gene transfections [6,7]. MNPs can also be used as magnetic resonance imaging (MRI) contrast agents to track the implanted cells, scaffold degradation, and bone regeneration.

This article reviews the state-of-the-art of new magnetic strategies for bone tissue engineering. First, the osteogenic effects of magnetic fields and MNPs were reviewed. Second, cutting-edge researches were described on magnetic strategies to improve the functions of cells and scaffolds, and to deliver genes, drugs and growth factors. Third, magnetic labeling for *in vivo* visualization and bone regeneration was also described.

2. Effects of magnetic field on bone tissue engineering

Magnetic fields include SMFs [8-11], pulsed electromagnetic fields (PEMFs) [12-15], rotating magnetic fields (RMFs) [16] and alternating electromagnetic fields [17]. They can help enhance the integration of implants with host tissues, increase the mineral density of newly-formed bone, and accelerate defect healing. Other applications of magnetic fields in bone tissue engineering were also being developed, including magnetically-assisted freezing

and thawing of stem cells [18-26], and magnetically-assisted scaffold and coating fabrications [27]. In particular, the combined application of magnetic fields with growth factors/drugs was able to achieve synergetic effects to substantially enhance bone regeneration [28-30].

The enhancing effects of magnetic fields were demonstrated on fracture-healing, spinal fusion, osteoarthritis, and wound-healing [1,3,4,11,31-34]. Magnetotherapy provided a non-invasive, safe, and easy method to treat the site of injury, the source of pain and inflammation, and other diseases. SMFs and PEMFs were the two most-studied types of magnetic fields. SMFs create a single magnetic field [35]. They received clinical applications with several therapeutic advantages. For example, by simply using a permanent magnet for tissue stimulation, a power device was not needed; this made SMF stimulation feasible for long-term bone healing [32]. SMFs have been categorized according to their intensity as ultra-weak (5 μT-1 mT), weak (1 mT), moderate (1 mT to 1 T), strong (1–5 T), and ultra-strong (> 5 T). Moderate intensity SMF was studied due to its easier realization in therapies [10]. Indeed, SMFs accelerated the proliferation, migration, orientation and differentiation of osteoblast-like cells [35-38], and induced the osteogenic differentiation of bone marrow-derived mesenchymal stem cells (BMSCs) [10,39].

The mechanism for these effects was likely because that the cell membrane possessed diamagnetic properties, and exposure to SMFs served to modify the membrane flux [40]. In addition, the extracellular matrix proteins had diamagnetic properties, and their structures and orientations could be affected by the SMF [41]. Indeed, animal studies showed that SMFs with moderate intensity increased the bone mineral density (BMD) and enhanced bone healing, including evidence in bone surgical invasion [42], ischemic bones [43], adjuvant

arthritis rats [44], ovariectomized rats [45], and bone grafts [46,47].

At the cellular level, SMFs could modulate cell functions [48], including the morphology, proliferation, cell cycle distribution, apoptosis, differentiation, gene expression, etc. Osteogenic differentiation was enhanced by the application of moderate SMFs for various types of cells, including BMSCs, human osteosarcoma cell lines MG63 [38], mouse calvarial osteoblast MC3T3-E1 [36], rat calvaria cells [35], human adipose-derived MSCs (hADMSCs) [49], and dental pulp stem cells (DPSCs) [50]. There were three likely mechanisms of SMF interactions with the cells: Electrodynamic interactions (Hall Effect); magnetomechanical interactions; and radical pair effects [8]. First, electrodynamic interactions are the first to be used to explain the bone mechano-adaptation. The Hall effect is from the variation in the streaming potential by SMF. The streaming potential is generated by strain gradients and ionic current flows along these microchannels when bone is subjected to a compression or mechanical deformation. SMF, which electrodynamically acts on any electric current or the moving and charged particles through electromagnetic induction, can affect the induced streaming potentials. Second, magnetomechanical effects are related to the uniformity of SMF and the inherent magnetic properties of materials. Bone is a tissue with an extremely small diamagnetic susceptibility. In a uniform magnetic field whose magnetic gradient is large enough, there is magnetic torque which makes the material with an anisotropy in the magnetic susceptibility to rotate until it reaches a stable orientation. Third, SMF can influence the rates of certain chemical reactions in biology due to the effect on the radical pair or electronic spin states of the reaction intermediates. The rate, yield or product distribution of the radical pair reactions can be altered by using an SMF with a modest or

weak intensity [8]**.** However, the exact mechanisms of SMF on the cells and the bone-healing enhancement still remain to be determined.

PEMFs produce magnetic fields and electric currents. Abundant evidence showed that PEMFs could accelerate fracture-healing and promote osteogenesis [33,51,52] and increase BMD [34]; in an ovariectomized (OVX) rat model, the application of PEMFs inhibited bone loss [53]. In addition, extremely low frequency (ELF)-PEMFs increased the osteogenic gene expressions in human alveolar bone-derived MSCs [54]. For example, at 50 Hz and in the range of 0.6-3.6 mT with exposure of 90 min/day, the 0.6 mT group was the best in stimulating the proliferation and osteogenic differentiation of rat calvarial osteoblasts [55]. Furthermore, histomorphometrical studies showed that PEMFs increased the new bone trabecular area, trabecular width, and trabecular number by 78%, 17% and 51%, respectively [56]. In addition, PEMFs reduced the trabecular separation by 44%, compared to the ovariectomy control rats [56].

Despite of the beneficial effects of PEMFs, the precise mechanisms are not yet fully understood. It was suggested that the osteogenesis-enhancement effects of PEMFs might be related with the induction of pulsed electric currents in bones to produce a sequence of biological cascades [57]. It was shown that PEMF exposure increased the cytosolic Ca^{2+} and activation of calmodulin, which were important factors associated with the mechanism of osteogenesis [58]. It was further shown that a 15 Hz and 1 mT treatment promoted the osteogenesis via MSCs [59]. In addition, the EMF-induced osteogenic markers were demonstrated to be mediated by signaling pathways including the protein kinase A (PKA) and the mitogen-activated protein kinase (MAPK) [59].

PEMFs could suppress the osteoclastic differentiation by modulating the pathways in the RANK/RANKL/OPG signaling system [60]. Furthermore, PEMF could modulate the osteoclastic differentiation via the Ca^{2+}-calcineurin-NFATc1 signaling pathway [13]. However, the suppressive regulatory effects of PEMFs on osteoclastogenesis might be less prominent and weaker than the enhancement effects on osteoblastogenesis. Indeed, PEMF exposure significantly increased the bone formation in an *in vivo* study, as revealed by the much greater mineral apposition rate, faster bone formation rate and larger osteoblast numbers (**Fig. 1**) [53]. PEMF exposure for 4 weeks promoted the skeletal gene expressions in Wnt/Lrp5/β-catenin signaling, confirming that the RANKL-RANK signaling served as a key pathway in the osteoclastic development and activation [61]. However, more efforts are still needed to elucidate the exact mechanisms of PEMFs on bone formation and to apply these mechanisms to clinical applications.

Other types of magnetic fields that could promote bone regeneration included nonpulsed sinusoidal electromagnetic fields [62], rotating magnetic fields [16], and combined magnetic fields (CMF) [63]. The latter also included dynamic sinusoidal magnetic fields and magnetostatic fields [63]. Moreover, efforts were made to compare the biological effects of SMFs with PEMFs. The results indicated that a moderate intensity of SMFs had more benefits than PEMFs for treating metabolic disorders, while PEMFs had more benefits than SMFs in treating musculoskeletal disorders and nerve functions [64]. PEMF can alter the cell membrane permeability through the induction of an electric field, thereby altering the cyclic guanosine monophosphate and cyclic adenosine monophosphate activity, and thus promoting osteogenesis [65]. On the other hand, SMF can neither produce electric currents nor create

vectorial changes. Instead, it can directly promote differentiation of osteoblasts and bone maturation via the aforementioned three possible mechanisms. Even for the same type of magnetic field, different parameters in intensity and frequency result in different magnetic fields. These different magnetic fields can induce different effects on the cells including the increase or decrease of the intracellular iron content [66]. Therefore, the cells respond differently to different magnetic fields. The cell proliferation depended on the stimulus intensity and duration of magnetic fields, cell type, cell age, and the treatment's "biological windows" [67]. A biological window refers to the range of the magnetic field at which the response of the biological system is significant. Magnetic field signals outside of the biological window would possess limited or no effects, or even negative or toxic effects. These important parameters require further study to determine and understand their effects on bone repair and regeneration. The biological effects of different types and various intensities and frequencies of magnetic fields for bone tissue engineering were summarized in Table 1.

3. Effects of MNPs on bone regeneration

3.1 Effects of SPIONs

MNPs, mainly superparamagnetic iron oxide nanoparticles (SPIONs), are promising for targeted imaging/drug delivery, tissue engineering, hyperthermia, gene therapy, and cell tracking applications. SPIONs can be taken up, exocytosed and metabolized by the cells. SPIONs alone, even without a magnetic field, were able to enhance the tissue repair efficacy [75], provide dynamic mechanical stimulations for bone formation [76], promote osteogenic differentiation of BMSCs [77], and enhance bone regeneration *in vivo* [78].

Furthermore, Huang et al. reported that Ferucarbotran, an ionic type of SPIONs, was not toxic to hMSCs, and was able to increase the cell growth [79]. The Ferucarbotran-promoted cell growth was because of the capability to suppress the intracellular H_2O_2 through an intrinsic peroxidase-like activity. In addition, Ferucarbotran enhanced the cell cycle progression, which could be modulated by the free irons (Fe) leached from the lysosomal degradation. The accelerated cell cycle progression involved the ability of Fe to alter the expression of the protein regulators [79].

To better understand the molecular mechanisms on why and how SPIONs promoted the osteogenic differentiation of MSCs, gene microarray assay and bioinformatics analyses were performed [77]. The results revealed that the gene expression was regulated, and the classic MAPK signal pathway was activated by the SPIONs. Therefore, the downstream genes of this pathway were modulated to enhance the osteogenic differentiation (**Fig. 2**) [77]. At the molecular level, SPIONs upregulated the long noncoding RNA INZEB2, which was critically important for sustaining the osteogenesis by MSCs. The overexpression of INZEB2 downregulated the ZEB2, a factor necessary to inhibit the BMP/Smad-dependent osteogenic transcription [80]. Thus, these results provided insights into the mechanisms of SPIONs at the molecular level, which could facilitate the application of SPIONs to enhance the regenerative medicine efficacy via stem cells.

In another study using a Sprague-Dawley rat model, SPION-containing gelatin sponges were implanted in the incisor sockets, which enhanced bone regeneration, with about 1.5-fold increases in BMD and bone volume per tissue volume (BV/TV), compared with gelatin sponge control without SPIONs [78]. As confirmed by immunohistochemistry and

transmission electron microscope (TEM) observations, the osteoblasts and vascular endothelial cells with SPIONs had greater osteogenic and angiogenic performances [78]. Therefore, the endocytic SPIONs promoted the osteogenic and angiogenic functions of the cells, leading to greater new bone formation [78].

3.2 Magnetic field-actuated SPIONs

SPIONs can be aligned by using an external magnetic field, and they can be randomized once the magnetic field is removed. However, in a colloidal suspension of SPIONs, the application of a magnetic field could cause the SPIONs to agglomerate [81]. The changes in physicochemical properties of the colloidal nanoparticles strongly influenced their biological properties. Hence, the agglomeration of SPIONs due to magnetic fields could alter their well-recognized biological impact. Indeed, reduction in cell uptake occurred because of the aggregation of the particles due to significant changes in both the size (from less than 100 nm to 300 nm) and zeta potential of the SPIONs [82]. In addition, external magnetic fields could influence the biological effects of SPIONs, because of changes in the size and surface charge governing the protein corona profile and the therapeutic/toxic effects [82]. Furthermore, the release of endocytic MNPs from the cells was suppressed by magnetic field, resulting in almost twice as much intracellular MNPs as those without a magnetic field [83]. The end result was that the more uptake of MNPs inside the cells, the greater the osteogenic differentiation of MSCs under the application of a magnetic field [83]. These findings were consistent with another study using (Fe^{2+}/Fe^{3+})-doped hydroxyapatite (FeHA) nanoparticles in cultures with osteoblast-like cells in the absence, or presence, of a SMF [84]. The FeHA

exposure to the magnetic field resulted in a significant increase in cell proliferation and greater osteoblastic activity due to the excellent biological properties of hydroxyapatite (HA) and the limited iron content [84]. Therefore, the changes in the physiochemical properties and endocytosis of the cells, induced by the MNPs under a magnetic field, could significantly enhance the cell behavior and bone regeneration capabilities.

4. Magnetically-modified cells for cell delivery, targeting and patterning

Stem cell-based therapies have great potential for tissue regeneration. MNP intake into the cells enables these cells to be controlled and manipulated by magnetic forces. Magnetic labeling is an attractive approach because of its technical simplicity, minimal toxicity and great labeling efficacy, especially for magnetic targeting. SPIONs could serve as an optimal labelling and tracer device for MSCs [85]. This section focuses on the applications of magnetically-labeled cells for bone tissue engineering, including cell targeting and cell patterning.

MSCs did not have substantial phagocytic capacity, thus restricting the intracellular uptake of SPIONs [86]. MNPs for cell labeling include Fe_3O_4, γFe_2O_3 and FeHA. To improve the biocompatibility and bioactivity, FeHA was fabricated by doping HA with Fe^{2+}/Fe^{3+} ions [87]. FeHA nanoparticles showed a number of important features as the magnetic ability and hyperthermia property were similar to those of magnetite or maghemite particles [87]. Suitable SPION sizes, surface modifications, concentrations and exposure time should be chosen to ensure minimal negative influence on cell function, maximum visibility and the longest duration [88].

MSCs could be labeled by modifying SPIONs which had more than 90% of efficiency in cell uptake without the use of a transfection agent [89,90]. For example, ferumoxytol was introduced into cells by producing ferumoxytol-heparin-protamine (HPF) complexes [91]. The idea was to create clusters of relatively larger nanoparticles (but still less than about 200 nm), which could be taken up more efficiently by the targeted cells. Combining protamine with ferumoxytol resulted in the formation of large, polydispersed complexes that were not incorporated into the cells. Although it would be counterintuitive to add heparin to protamine/ferumoxytol to facilitate endosomal incorporation in the cells, the addition of heparin gave rise to the formation of HPF nanocomplexes that were endocytosed by the cells [91]. Other strategies in adjusting endocytosis of SPIONs included the passive targeting or active targeting of cells [92]. Passive targeting employed SPIONs which were functionalized by placing a surface coating. Testing SPIONs as contrast agents for pathological applications, clinical trials currently underway predominantly used passive SPIONs. There were two types of surface coatings in passive targeting: (i) inorganic shells, including Au/Ag [93], Gd, Zn [94], Ni [95], Ni silicate [95], quantum dot shell [96], graphene [97], and silica; and (ii) organic shells, containing surfactants, dendrimers, polymers and blends of polymers [98-104]. On the other hand, active targeting used a moiety to guide the functionalized SPIONs moving toward the targeted pathological position [105-107]. Several targeting moieties were tested, most of which using oligomers, drugs, proteins, peptides, and aptamers which were functional peptides or oligonucleotides that could connect to various chemical and biological molecules with good affinity and selectivity. SPIONs were coupled to various targeting moieties and employed as a platform to target receptors [108], enzymes [109], integrins [110]

and specific kinds of cells [111].

A novel method was reported on surface functionalization of MNPs with biocompetent dendrons that significantly improved the magnetization of hBMSCs [99]. The interaction between BMSCs with MNPs having a thin coating of poly(acrylic acid) (PAA) was achieved through functionalization of the PAA using hyperbranched poly(epsilon-lysine) dendrons. The rationale for this method was that the high-density presentation of this hydrophilic amino acid could enhance the interaction between the cell surface glycocalyx and MNPs, thus promoting the cells to internalize more MNPs [99]. In this way, the functionalized MNPs significantly enhanced the efficiency of MNP adhesion to the cell membrane and their subsequent internalization. This in turn resulted in the rapid (15 min) and efficient (80%) magnetization of the primary hBMSCs in the suspension, and avoiding the need for the additional step of adhesion culture [99].

Accurate cell guidance and cell retention in the targeted wound site are a major challenge for cell therapy. To this end, magnetic cell-targeting methods represent a promising approach. SPION-labeled cells could be driven by a magnetic field to localize at the target site where they would perform their functions to maximize the therapeutic/diagnostic effects [112]. In animal studies, the transplantation of BMSCs indeed showed meritorious effects after spinal cord injuries [113]. Intravenous injection was the least invasive, compared to direct injection and lumbar puncture. Its efficiency could be remarkably increased using magnetically-labeled cells with the assistance of magnetic fields. In a magnetic targeting study of BMSCs in a rat spinal cord injury model, magnetically-labeled BMSCs were injected into the subarachnoid space [113]. In the magnetic group, substantial BMSC

aggregations were discovered on the surface of the injured spinal cord; in comparison, few BMSCs were discovered in the nonmagnetic control group [113]. In addition, autogenic transplantation of magnetically-labeled MSCs were used to repair severe chronic osteochondral defects, with a 10-min exposure to a magnetic device, achieving a significantly better repair of chronic defects, successfully producing new chondrogenic tissues [114]. These results are consistent with another study showing an accumulation of MSCs at the wound site, resulting from the use of a magnetic field to increase the speed of cell transport [112]. Therefore, using magnetic forces promoted the homing and guided the magnetized stem cells to make rapid directional movements, thus enhancing the efficacy of stem cell-targeted therapies.

Besides manipulating the magnetic cells, magnetic nanotechnology could be used to manipulate osteogenic mechanosensitive receptors, thus inducing osteoprogenitor cell differentiation into the osteogenic lineage. Kanczler et al. investigated the magnetic field activation of MNPs tagged on the mechanosensitive receptors of hBMSC membranes. The stimulation of MNP-labeled hBMSCs indeed enhanced the expression of osteogenic genes, producing 2-fold increases in RUNX2 and OPN *in vitro*, along with greater production of proteoglycans and collagen *in vivo* [115].

Another important application of magnetic cells was that the magnetic cells could be patterned by magnetic forces to fabricate scaffold-free cell-sheets, which was a promising strategy for stem cell transplantation and therapy. The cell-to-cell junctions and secretion of extracellular matrix (ECM) proteins maintained the cell-sheets [116,117], which were thus similar to natural tissues. Compared with non-magnetic cell-patterning approaches such as

cell-laden hydrogels, three-dimensional (3D) printing, inkjet printing and laser-assisted bioprinting [118], the magnetic method was more versatile and had greater multifunctionality [119]. For example, MNPs and magnetic fields could be used to position the cells in a pattern suitable for tissue engineering. These magnetically-labeled cells were accumulated in a desired pattern through a magnetic field below a cell culture surface [120]. In this way, it was feasible to control the cell packing density by tuning the magnetic field gradient and intensity [120]. This ability to control the cell density and cell distribution is expected to be highly beneficial to promote the regeneration of various tissues.

Furthermore, growth-factor-localized cell sheets were fabricated via magnetic patterning [121]. In this system, specific cells and growth factors in each layer of the cell sheets were accurately controlled by magnetic-force-mediated deposition (**Fig. 3**). Based on the histological properties of tissues in vivo, the 3D distribution of cells and proteins were maintained in the artificial micro-tissues, in addition to sustaining the form that could be fitted into specific defects. To control both cells and proteins, new Fe_3O_4 MNPs were developed that were coated with nanoscale graphene oxide (nGO@Fe_3O_4) [121]. With the help of these MNPs, bone morphogenetic protein 2 (BMP2) was incorporated into the cell sheets to induce bone formation, achieving much greater phosphorylation of Smad1/5/8 signaling. Moreover, the construction of an integrated osteochondral complex was also achieved using a combination of DPSCs/TGFβ3 and DPSCs/BMP2 [121]. This method successfully induced the DPSC differentiation into both mCherry+ chondrocytes and GFP+ osteoblasts, and their distribution was consistent with the distribution of the specific growth factors that were respectively inducing these cells [121]. Therefore, this novel magnetic

approach has great potential to benefit osteochondral defect regeneration with different types of layered tissues.

5. Magnetic scaffolds fabrication and their effects in bone tissue engineering

5.1 Fabrication of magnetic scaffolds and their performance without using a magnetic field

The simplest way to obtain magnetomechanically-functional scaffolds was to dip-coat the scaffolds into aqueous ferrofluids containing SPIONs coated with various biopolymers [122-125]. After dip-coating, the nanoparticles were integrated into the porous structure of the scaffolds. This method was used to turn HA and collagen scaffolds into magnetic scaffolds [122]. These magnetic scaffolds could support the adhesion and proliferation of hBMSCs, and had no negative influence on osteoblastic differentiation [122]. These results were consistent with another study on MNP-HA magnetic scaffolds with various MNP contents (from 0.2% to 2%) by immersing the HA scaffold into MNP colloidal solutions [123].

Another approach incorporated the MNPs into the scaffold with dispersion throughout the scaffold [123-140]. The fabrication methods included: co-electrospinning [126-131], rapid prototyping technique [132,133], *in situ* nucleating [134], foam replication technique [135], chemical reaction between a solid and a liquid [136,137], freeze-drying [138,139], evaporation-induced self-assembly (EISA) [140-142], and solvent-casting techniques [143]. Electrospinning had advantages including a high surface area/volume ratio, potential for the release of drugs and antimicrobials, controllable fiber diameters, high porosity and

permeability. Meng et al. fabricated paramagnetic nanofibrous γ-Fe_2O_3/nHA/polylactic acid (PLA) composite films [126]. This new material increased the proliferation of osteoblastic cells by about 2 folds due to the SPION incorporation [126].

In a recent study, SPIONs were incorporated into an injectable calcium phosphate cement (CPC) scaffold by mixing the CPC powder with a SPION solution [136]. The addition of SPIONs caused substantially better hDPSC attachment and spreading, and a 3-fold increase in osteogenic differentiation, compared to that without SPIONs. The bone matrix mineral synthesis by the cells was also increased by 2-3 folds, compared to that without SPIONs (**Fig. 4**). The reason for this enhancement was attributed to the improved microstructure of the scaffold containing SPIONs, and the release and internalization of the incorporated SPIONs by the cells [136].

Furthermore, magnetic scaffolds were also prepared via 3D printing of Fe_3O_4 nanoparticle-containing bioactive glass/polycaprolactone (Fe_3O_4/MBG/PCL) scaffolds [133]. 3D fully-biodegradable magnetic scaffolds were made using PCL matrix and FeHA nanoparticles [132]. The cell growth on the magnetized scaffolds was 2.2-fold greater than that in non-magnetized control [132]. In a rabbit model, the PCL/FeHA scaffolds were completely filled with new bone at 4 weeks, while the non-magnetized control had much less new bone formation [132]. Because the PCL/FeHA scaffolds were designed to yield a cellular microenvironment feasible for bone regeneration and to produce a magnetic field using an external magnetic power. Therefore, the loading and the growth of seed cells was greatly enhanced.

MNPs were also immobilized on the scaffold surface by electrostatic layer-by-layer

(LbL) assembly, which formed multilayer films based on the alternative adsorption of oppositely charged polyelectrolytes, inorganic nanoparticles, macromolecules, and even supramolecular systems on the charged substrates [144]. Tang et al. reported LbL assembly of silica nanoparticles on fiber surfaces of 3D fibrous scaffolds, which enhanced osteoblast cell attachment, proliferation, and ALP activities due to the increased surface roughness and wettability [145]. More recently, a novel magnetic poly(lactic-co-glycolic acid) (PLGA)/PCL scaffold was developed via a combination of electrospinning and LbL assembly of SPIONs [146]. Magnetic nanogranular interface on the PLGA/PCL scaffold was constructed instead of simply mixing the MNPs with the polymer. With this novel interface, the osteogenic differentiation of ADSCs was greatly enhanced by over 2 folds. By comparison with gold nanoparticles, the enhanced effect of the magnetic PLGA/PCL scaffold was considered to result from the magnetic effect, rather than the presence of nanoparticles and the increased surface roughness (**Fig. 5**) [146].

Magnetic fields were used to assist in the scaffold fabrication process [147-151]. The directional movement of MNPs was controlled by magnetic fields, thus enabling precisely-controlled fabrication of magnetic fibrous scaffolds [147], multilayer grids formation by alignment of SPIONs/poly(vinyl alcohol) (PVA) nanofibers, and fibrous bundle formation using SPIONs and PLGA nanofibers [148]. Li et al. combined the membrane assembly with magnetic forces to preserve the mechanical integrity and interconnectivity of 3D scaffolds [139]. An ordered and layered structure was achieved using a magnetic technique through the addition of MNPs into PCL/gelatin nanofibers. Scaffolds from the magnetically-guided fabrication strategy had the potential to mimic the structures and

functions of human tissues [149]. In addition, because these scaffolds could be easily and repeatedly assembled and un-assembled, they could facilitate the study of cell-cell interactions in a controllable 3D environment [152]. Currently-available magnetic scaffolds and their properties without using magnetic fields were summarized in Table 2.

5.2 Magnetic scaffolds with the application of magnetic fields

Further enhancement in osteogenic differentiation and bone regeneration was achieved by combining magnetic scaffolds with magnetic fields [70, 152-157]. Meng et al. prepared a nanofibrous scaffold using SPIONs, nHA and PLA [126,156]. The scaffold was implanted in the lumbar transverse defects in rabbits. Magnets were placed in the rabbit cages to maintain a SMF after the surgery. The MNP scaffold induced greater new bone and remodeling in the rabbit defects. These results validated the *in vivo* osteogenesis enhancement by the super-paramagnetic nano-fibrous scaffold with the synergistic application of an SMF (**Fig. 6A-E**) [156].

More recently, Yun et al. investigated the combined effects of SMF with a PCL-MNP nanocomposite scaffold on osteoblastic functions and bone formation (**Fig. 6F**). The synergy between magnetic scaffold and magnetic force was manifested in the initiation of integrin signaling pathways, including focal adhesion kinase, paxillin, RhoA, MAPK, and nuclear factor-kappaB (NF-κB), and in promoting bone morphogenetic protein-2 and phosphorylation of Smad1/5/8 [157]. The combination of SMF and magnetic scaffold also enhanced the angiogenesis via endothelial cells, resulting in greater expressions of vascular endothelial growth factor and angiogenin-1 genes, and promoting the synthesis of capillaries (**Fig. 6G**).

When the magnetic scaffolds were implanted in mouse calvarium defects, the application of SMF significantly enhanced the new bone formation at 6 weeks. Compared to the 0% MNP scaffolds, the bone volume in the 10% MNP scaffold without SMF was increased by 1.9 times [157]. With the application of a SMF and the 10% MNP scaffold, the bone volume was increased by 2.7 times [157]. The reason for this increase in new bone was attributed to the synergy of the integrin, BMP, MAPK and NF-κB signaling pathways in the osteoblasts by culturing with SMF and the magnetic scaffolds [157]. Therefore, the combined application of an external magnetic field and magnetic scaffold might synergize the magnetism effects on the cells and thus might be a useful platform for bone tissue engineering.

Another benefit of magnetic fields was that higher cell-seeding efficiency could be achieved using magnetic forces to attract the SPION-labeled cells and prevent them from flowing away. In this way, more cells could be seeded into the pores of the scaffolds. This novel cell-seeding method resulted in a cell seeding efficiency of three folds higher than that of conventional passive seeding [158]. Indeed, the combined use of magnetic cells and magnetic forces not only increased the number of scaffold-adherent cells, but also enhanced the cell infiltration and distribution, compared with control [159]. Moreover, the magnetic cell seeding method enhanced the osteogenic differentiation of the stem cells [160]. At 14 days, the levels of ALP and osteocalcin (OCN) for the magnetic cell seeding group were significantly higher than those of static-seeding, which may be due to the cellular activity or the increased total number of cells in the scaffolds [160]. Currently-available studies involving magnetic scaffolds with the use of magnetic fields for osteogenesis were summarized in Table 3.

6. Magnetic strategies for growth factor and drug delivery

The mechanism of bone repair is complex and involves several important growth factors and small molecules, such as BMP-2, platelet-derived growth factor (PDGF) and parathyroid hormone (PTH). These molecules can act directly to positively influence the bone mass, or indirectly, by acting on negative regulators (i.e., inhibitors) of the bone mass [165]. Therefore, delivering growth factors is an important approach in bone tissue engineering, in addition to the use of stem cells and scaffolds.

MNPs served as delivery vehicles for bioactive agents such as drugs, chemotherapeutics, antibodies, peptide therapeutics, oligonucleotides, and growth factors via magnetic fields [166-170]. Growth factors could be stabilized by conjugation to nano-constructs [171]. The growth factors immobilized to iron oxide/human serum albumin nanoparticles promoted a higher growth and differentiation of the cells, compared to their counterparts [166]. When applied in the deeper parts of the body, the efficiency of capturing MNPs was ensured by the use of a remnant magnetic implant especially when the external magnetic field was turned off [172], which was a major advantage of magnetic delivery systems.

MNPs could be used to target mechanically-responsive receptors, such as the TREK1 ion channel, PDGF receptors and integrins [173,174], and Wnt receptor [175]. They enabled the ligand-MNP complex to be manipulated using magnetic fields, allowing the control of ion channel stimulation. The osteogenesis of hMSCs could be significantly enhanced by mechanical stimulation via magnetic tagging. The application of magnetic activation was capable of initiating nuclear translocation of β-catenin to a similar level as Wnt3a, which

enhanced the skeletal progenitor cell proliferation, differentiation and accelerated bone repair in Axin2 knockout mice [176]. By initially targeting the cell membrane receptor PDGFRα, a higher mineral content was present in the cells after 3 weeks of magneto-mechanical stimulation and osteogenic medium culture [174].

Magnetic iron oxides and gold nanoparticles were embedded in nanoshuttle which was used as a drug carrier for human cells [168]. The drug release inside the cells could be controlled by applying heat and a magnetic field. Moreover, the use of the magnetic field to pull the nanoshuttle is promising for tissue-specific clinical applications in bone, heart, lung and brain, for targeted drug delivery and on-demand drug release. Furthermore, the magnetic targeting method enhanced the viral and non-viral gene delivery [7]. This strategy was applied to a range of viral vectors (including adenoviruses, adeno-associated viruses and lentiviruses) [177], cationic polymers (polyethyleneimine, or PEI) [178], as well as cationic lipids [179]. Compared with common transfection approaches, a key advantage of the magnetic targeting method was the lower dosage of the vector, which could be applied both *in vitro* and *in vivo*. Moreover, due to the high target site specificity, side effects for viral or non-viral gene delivery were also lowered.

For magnetic transfection, various polymers, lipids, and dendrimers were developed to prepare MNPs with accurate sizes, shapes, compositions, magnetization, relaxivity and surface charge [180-182]. Several PEI-coated MNPs for efficient transfection are commercially available, for example, Polymag™ and CombiMag™ (OZ Biosciences, Marseille, France). By using chemisorption through van der Waals forces, high molecular weight PEI was bonded with MNPs. In this way, a transfection efficacy similar to commercial

transfection agents (Lipofectamine™ 2000 and Polymag) was achieved, with higher DNA binding capacity, less PEI, and reduction of toxicity [183]. The MNP-bound polyplexes were likely responsible for the greater gene transfer efficacy and the minimal cytotoxicity.

Besides PEI, 3-Aminopropyl triethoxysilane (APTES)-modified SPIONs also demonstrated substantial promise for gene delivery for DNA and siRNA molecules, when the APTES-modified SPIONs were used together with cationic polymers such as Lipofectamine and TurboFect [180]. This increased the gene-binding capacity, protected the genes from degradation, and improved the gene transfection efficiency for DNA and siRNA in both adherent and suspension cells [180]. When combined with a MSC-targeting peptide, magnetic nanoclusters could deliver a gene to MSCs at a higher efficiency than commercial vectors. The magnetic properties could promote the delivery and aid in magnetically-guided gene delivery, which would be crucial for future *in vivo* applications [182].

Magnetic liposomes are lipid-based nanoparticles containing magnetic substances. They are useful for delivery of drugs and genes due to their dual hydrophilic-hydrophobic domains and magnetic properties [179]. The lipid bilayer of liposomes loaded with MNPs could be disrupted by short magnetic pulses to achieve the fast release of the liposomes' payload without a significant increase in local temperatures [184]. Novel thermosensitive cationic magnetic liposomes (TSMCLs) consisted of 1,2-Dipalmitoyl-sn-glycero-3-phosphocholine (DPPC), 3ß-[N-(N', N'-dim-ethylaminoethane)-carbamoyl] cholesterol (DC-Chol), Dimethyldioct-adecylammonium bromide (DOAB) and cholesterol at a molar ratio of 80:5:5:10. TSMCLs were developed with 0.5 mg/mL magnetic fluid Fe_3O_4. TSMCLs showed feasible temperature sensitivity and magnetic responsiveness, and demonstrated great

efficacy for co-delivering drugs and genes using the application of an alternating magnetic field [185]. MNPs could be the stimulator to induce small molecule release from the liposomal delivery. Nakayama et al. used SPIONs to trigger the opening of mechanosensitive channels of large conductance (MscL) nanovalves [186]. Due to their large open pores, the MscL channels presented a promising nanovalve delivery vehicle for liposomal drugs [186].

To increase the cell targeting capacity, the MNP-liposome complexes were associated with transferrin [187]. Pan et al. synthesized cationic lipid-coated MNPs and prepared transferring-coated MNP/(PEI/Plasmid DNA) complexes [187]. The transfection using these magnetic vectors required much less incubation time in the presence of an external magnetic field, and achieved gene transfer at a high efficiency [187]. Therefore, magnetic delivery and gene transfection would be an important future research focus, with the purpose to reduce the side effects of a specific drug for treating bone diseases, and to enhance the treatment by endogenous growth factors.

The magnetic liposomes had multiple functions, including imaging and therapy, with magnetic field, ultrasound, and MRI. Liu et al. designed multifunctional magnetic nanoliposomes [188]. SPIONs with a diameter of about 7 nm were encapsulated in the aqueous core of the 200 nm diameter liposomes, with hydrophobic anethole ditholethione (ADT) doped in the phospholipid shell. The specific intra-tumoral accumulation and distribution were dynamically monitored by MRI. Meanwhile, with ADT molecule release (organic hydrogen sulfide H_2S donors) in the tumor matrix, great amounts of microsized bubbles of H_2S were produced continuously by using an enzymatic trigger. At the same time, real-time ultrasound imaging was employed to evaluate the production process of the H_2S

microbubbles. Furthermore, when directed by ultrasound imaging, the H_2S microbubbles acted like an intra-tumoral bomber. It could explode to ablate the local tumor tissue when applying a higher acoustic intensity for bubble cavitation. The rupture of the microbubbles and the diffusion of high densities of H_2S molecules into the deep areas inside the tumors substantially promoted the anti-tumor effect (**Fig. 7**) [188]. Thus, magnetic gene delivery systems could be multifunctional, performing functions that include the diagnosis, treatment and visualization of the disease simultaneously. Therefore, magnetic gene delivery is very promising for stem cell-based tissue engineering applications.

7. Magnetic labeling for *in vivo* visualization

Stem cell-based *in vivo* tracking is mostly applied to cardiovascular, brain and kidney systems. More recently, stem cell-based *in vivo* tracking was also used for bone regeneration [85]. Generally, the prerequisite was that the osteogenic differentiation of MSCs was not negatively affected by SPION-labeling [80,189,190]. SPIONs in conjunction with MRI have been widely used to image and track MSCs *in vivo* in a non-invasive manner [191-193]. A study reported that the SPION-labeled BMSCs were tracked to evaluate the migration and prognosis in an animal cartilage defect model [193]. Obvious changes in signal in the defect region after surgery on SET2-weighted MR image were found and persisted till 24 weeks after implantation of SPION-labeled BMSCs mixed with type II collagen hydrogel transplanted to cartilage defect in a minipig model. This would show the distribution and diffusion of the labeled cells, thereby elucidating the regenerative mechanisms and providing opportunities to improve the current repair strategies [193].

To enhancing the labelling and homing efficiency to the target site, MNPs of special structure and component were designed and prepared. Huang et al. fabricated an iron-based nanocluster by combining zinc-doped iron oxide ($Zn_{0.4}Fe_{2.6}O_4$) with hyaluronic acid-cholanic acid amphiphilic polymer [194]. Zinc-doped iron oxide MNPs had greater effect for T2 MR imaging contrast when compared to the Fe_3O_4 and Feridex without zinc [195,196]. Hyaluronic acid coating could promote the interactions with CD44, which is a specific cell surface receptor of MSCs [197]. The hyaluronic acid coating resulted in highly effective cellular uptake of the hyaluronic acid-$Zn_{0.4}Fe_{2.6}O_4$ nanocluster. The iron content in the $Zn_{0.4}Fe_{2.6}O_4$ increased the chemokine receptor CXCR4 expression in MSCs, which could enhance the homing of MSCs to the target site [194].

In addition to labeling the stem cells, directly labeling the scaffold materials could be more beneficial, more informative, and easier to translate to clinical applications [198]. Ganesh et al. reported the incorporation of multifunctional nano HA (MF-nHA) particles, within an electrospun PCL nanofibrous scaffold [153]. The PCL/MF-nHA scaffolds were mechanically stronger than the PCL/nHA scaffolds. They promoted the proliferation and improved the early osteogenic differentiation of hMSCs. Most importantly, the PCL/MF-nHA scaffolds are MR-visible [153]. The amount of SPIONs incorporated into the scaffolds was correlated to the MR signal intensity, and the scaffold degradation could be visualized using MRI [198].

Investigating the process of bone reconstruction on the implanted scaffold in the defect remains a changeling. Methods such as combining MRI with fluorescence imaging, probe-based confocal laser endomicroscopy (pCLE), NIR optical imaging, or micro CT could

be used to perform the evaluation non-invasively [199,200]. These methods enabled the analyses including implant positioning, inflammation divulgement, implant resorption, new trabeculae, bone texture, and other quantitative measurements [201]. For example, gelatin sponges loaded with SPIONs (SPION-GS) were implanted in the incisor sockets of Sprague-Dawley rats [78]. A significant decrease in the signal intensity of T2-weighted MRI in the SPION-GS group was found than the control. The scaffold degradation and interactions with host tissues would cause changes in the image intensity, which could be monitored over time visually (**Fig. 8**). Micro CT showed that the SPION-GS group had more new bone and a better-preserved alveolar ridge than blank control group at 4 weeks. Because of the rapid degradation of GS, the number of SPIONs was lowered quickly with time, while the number of endocytic SPIONs in the cells was increased over time. The MRI successfully detected the these residual SPIONs along with the newly-formed bone at 4 weeks. These results indicated that the SPIONs indeed enhanced the osteogenesis [78]. This method has the potential to meet the need for non-invasive monitoring the repair process *in vivo* and enhancing the bone regeneration efficacy simultaneously.

8. Conclusions and future perspectives

Increasing amounts of experimental data indicate the great potential of magnetic strategies for bone tissue engineering. The current cutting-edge research involving magnetically-assisted bone tissue engineering approaches was summarized into the following four aspects.

First, there were many studies on the application of PEMF alone in bone engineering,

likely due to the more variable settings, compared to SMF. There were also many studies on the combination of SMF with scaffolds. Moderate intensities of SMFs could induce the most significant and beneficial biological effects, compared to other types of SMFs.

Second, for free MNPs, the responses were greater when the MNPs were internalized into the cells rather than attached to the cells' external surfaces. When incorporated into the scaffolds, different distribution of MNPs inside the scaffold would lead to incongruous gradients of magnetic moment and thus producing distinct effects on cell activity. Homogeneous distribution resulted in faster bone regeneration but relatively immature new bone. On the other hand, an inhomogeneous distribution resulted in a higher level of bone maturity but with less new bone formation.

Third, molecular mechanisms of the effect of magnetic induction at the body temperature involved the activation of signaling such as the Wnt/β-catenin and integrin signaling pathways (including focal adhesion kinase, paxillin, RhoA, MAPK, and NF-κB), as well as in the up-regulation of BMP-2 and phosphorylation of Smad1/5/8. In addition, the angiogenic responses of endothelial cells were promoted, including the expression of vascular endothelial growth factor (VEGF) and angiogenin-1 genes, as well as the formation of capillary tubes and blood vessels.

Fourth, with iron-based magnetic scaffolds, there were debates on whether it was the physical effects or the chemical effects that evoked the biological effects. However, the biological effects should be due to both chemical (e.g., Fe^{2+}) and physical effects (e.g., magnetic forces). Carefully-designed experiments using non-magnetic iron oxide are needed to determine each effect separately and to reveal the underlying mechanisms.

Moreover, future work should be focus on the following three aspects. First, more studies are needed on the combined applications of magnetically-enhanced cells and magnetic scaffolds, together with *in vivo* non-invasive tracking of the implanted stem cells, scaffold degradation and bone regeneration. Second, studies are needed to determine the biological effects of power frequency (50 Hz and 60 Hz) EMF alone and in combination with MNPs and magnetic scaffolds. Third, the bio-safety issues of the applications of magnetic strategies in bone tissue engineering warrant further investigation. To date, *in vivo* histological studies reveal no serious inflammation or toxic effects; however, these studies were relatively short-term. The effects of SPIONs *in vivo* need to be thoroughly investigated via long-term studies.

Reference

1. Xu HY, Gu N. Magnetic responsive scaffolds and magnetic fields in bone repair and regeneration. Frontiers of Materials Science. 2014; 8:20-31.

2. Chung E, Sampson AC, Rylander MN. Influence of heating and cyclic tension on the induction of heat shock proteins and bone-related proteins by MC3T3-E1 cells. Biomed Res Int. 2014; 2014: 354260.

3. Quittan M, Schuhfried O, Wiesinger GF, Fialka-Moser V. Clinical effectiveness of magnetic field therapy--a review of the literature. Acta Med Austriaca. 2000; 27:61-8.

4. Gujjalapudi M, Anam C, Mamidi P, Chiluka R, Kumar AG, Bibinagar R. Effect of magnetic field on bone healing around endosseous implants - An in-vivo study. J Clin Diagn Res. 2016; 10: ZF01-4.

5. Zhao X, Kim J, Cezar CA, Huebsch N, Lee K, Bouhadir K, et al. Active scaffolds for on-demand drug and cell delivery. Proc Natl Acad Sci U S A. 2011; 108: 67-72.

6. Singh D, McMillan JM, Kabanov AV, Sokolsky-Papkov M, Gendelman HE. Bench-to-bedside translation of magnetic nanoparticles.Nanomedicine (Lond). 2014; 9: 501-16.

7. Delyagina E, Li W, Ma N, Steinhoff G. Magnetic targeting strategies in gene delivery. Nanomedicine (Lond). 2011; 6: 1593-604.

8. Zhang J, Ding C, Ren L, Zhou Y, Shang P. The effects of static magnetic fields on bone. Prog Biophys Mol Biol. 2014; 114: 146-52.

9. Zhang J, Ding C, Shang P. Alterations of mineral elements in osteoblast during differentiation under hypo, moderate and high static magnetic fields. Biol Trace Elem Res. 2014; 162: 153-7.

10. Kim EC, Leesungbok R, Lee SW, Lee HW, Park SH, Mah SJ, et al. Effects of moderate intensity static magnetic fields on human bone marrow-derived mesenchymal stem cells. Bioelectromagnetics. 2015; 36: 267-76.

11. Bambini F, Santarelli A, Putignano A, Procaccini M, Orsini G, Di Iorio D, et al. Use of supercharged cover screw as static magnetic field generator for bone healing, 2nd part: in vivo enhancement of bone regeneration in rabbits. J Biol Regul Homeost Agents. 2017; 31: 481-5.

12. Daish C, Blanchard R, Fox K, Pivonka P, Pirogova E. The application of pulsed electromagnetic fields (PEMFs) for bone fracture repair: past and perspective findings. Ann Biomed Eng. 2018; 46: 525-42.

13. Zhang J, Xu H, Han Z, Chen P, Yu Q, Lei Y, et al. Pulsed electromagnetic field inhibits RANKL-dependent osteoclastic differentiation in RAW264.7 cells through the Ca^{2+}-calcineurin-NFATc1 signaling pathway. Biochem Biophys Res Commun. 2017; 482: 289-95.

14. Selvamurugan N, He Z, Rifkin D, Dabovic B, Partridge NC. Pulsed electromagnetic field regulates microRNA 21 expression to activate TGF-β signaling in human bone marrow stromal cells to enhance osteoblast differentiation. Stem Cells Int. 2017; 2017: 2450327.

15. Zhu S, He H, Zhang C, Wang H, Gao C, Yu X, et al. Effects of pulsed electromagnetic fields on postmenopausal osteoporosis. Bioelectromagnetics. 2017; 38: 406-24.

16. Pan X, Xiao D, Zhang X, Huang Y, Lin B. Study of rotating permanent magnetic field to treat steroid-induced osteonecrosis of femoral head. Int Orthop. 2009; 33: 617-23.

17. Creecy CM, O'Neill CF, Arulanandam BP, Sylvia VL, Navara CS, Bizios R. Mesenchymal stem cell osteodifferentiation in response to alternating electric current. Tissue Eng Part A. 2013; 19: 467-74.

18. Lee SY, Huang GW, Shiung JN, Huang YH, Jeng JH, Kuo TF, et al. Magnetic cryopreservation for dental pulp stem cells. Cells Tissues Organs. 2012; 196: 23-33.

19. Kojima SI, Kaku M, Kawata T, Motokawa M, Sumi H, Shikata H, et al. Cranial suture-like gap and bone regeneration after transplantation of cryopreserved MSCs by use of a programmed freezer with magnetic field in rats. Cryobiology. 2015; 70: 262-8.

20. Wang J, Zhao G, Zhang Z, Xu X, He X. Magnetic induction heating of superparamagnetic nanoparticles during rewarming augments the recovery of hUCM-MSCs cryopreserved by vitrification. Acta Biomater. 2016; 33: 264-74.

21. Koseki H, Kaku M, Kawata T, Kojima S, Sumi H, Shikata H, et al. Cryopreservation of osteoblasts by use of a programmed freezer with a magnetic field. Cryo Letters. 2013; 34: 10-9.

22. Iwasaka M, Onishi M, Kurita S, Owada N. Effects of pulsed magnetic fields on the light scattering property of the freezing process of aqueous solutions. J Applied Physics. 2011;109: 07E320.

23. Lee SY, Chiang PC, Tsai YH, Tsai SY, Jeng JH, Kawata T, et al. Effects of cryopreservation of intact teeth on the isolated dental pulp stem cells. J Endod. 2010; 36: 1336-40.

24. Lin PY, Yang YC, Hung SH, Lee SY, Lee MS, Chu IM, et al. Cryopreservation of human embryonic stem cells by a programmed freezer with an oscillating magnetic field. Cryobiology. 2013; 66: 256-60.

25. Kojima S, Kaku M, Kawata T, Sumi H, Shikata H, Abonti TR, et al. Cryopreservation of rat MSCs by use of a programmed freezer with magnetic field. Cryobiology. 2013; 67: 258-63.

26. Shikata H, Kaku M, Kojima SI, Sumi H, Kojima ST, Yamamoto T, et al. The effect of magnetic field during freezing and thawing of rat bone marrow-derived mesenchymal stem cells. Cryobiology. 2016; 73: 15-9.

27. Zhao X, He J, Zhang J, Wang X, Wang W. The effect of magnetic field on electrochemically deposited calcium phosphate/collagen coatings. Biomed Mater Eng. 2014; 24: 1851-9.

28. Okada M, Kim JH, Yoon ST, Hutton WC. Pulsed Electromagnetic Field (PEMF) plus

BMP-2 upregulates intervertebral disc-cell matrix synthesis more than either BMP-2 alone or PEMF alone. J Spinal Disord Tech. 2013; 26: E221-6.

29. Wang T, Wang P, Cao Z, Wang X, Wang D, Shen Y, et al. Effects of BMP9 and pulsed electromagnetic fields on the proliferation and osteogenic differentiation of human periodontal ligament stem cells. Bioelectromagnetics. 2017; 38: 63-77.

30. Kapi E, Bozkurt M, Selcuk CT, Celik MS, Akpolat V, Isik FB, et al. Comparison of Effects of Pulsed Electromagnetic Field Stimulation on Platelet-Rich Plasma and Bone Marrow Stromal Stem Cell Using Rat Zygomatic Bone Defect Model. Ann Plast Surg. 2015; 75: 565-71.

31. Cho H, Choi YK, Lee DH, Park HJ, Seo YK, Jung H, et al. Effects of magnetic nanoparticle-incorporated human bone marrow-derived mesenchymal stem cells exposed to pulsed electromagnetic fields on injured rat spinal cord. Biotechnol Appl Biochem. 2013; 60: 596-602.

32. Aydin N, Bezer M. The effect of an intramedullary implant with a static magnetic field on the healing of the osteotomised rabbit femur. Int Orthop. 2011; 35: 135-41.

33. Petecchia L, Sbrana F, Utzeri R, Vercellino M, Usai C, Visai L, et al. Electro-magnetic field promotes osteogenic differentiation of BM-hMSCs through a selective action on $Ca^{(2+)}$-related mechanisms. Sci Rep. 2015; 5: 13856.

34. Shen WW, Zhao JH. Pulsed electromagnetic fields stimulation affects BMD and local factor production of rats with disuse osteoporosis. Bioelectromagnetics. 2010; 31: 113-9.

35. Yamamoto Y, Ohsaki Y, Goto T, Nakasima A, Iijima T. Effects of static magnetic fields on bone formation in rat osteoblast cultures. J Dent Res. 2003; 82: 962-6.

36. Ba X, Hadjiargyrou M, DiMasi E, Meng Y, Simon M, Tan Z, et al. The role of moderate static magnetic fields on biomineralization of osteoblasts on sulfonated polystyrene films. Biomaterials. 2011; 32: 7831-8.

37. Cunha C, Panseri S, Marcacci M, Tampieri A. Evaluation of the effects of a moderate intensity static magnetic field application on human osteoblast-like cells. American Journal of Biomedical Engineering. 2012; 2: 263-8.

38. Feng SW, Lo YJ, Chang WJ, Lin CT, Lee SY, Abiko Y, et al. Static magnetic field exposure promotes differentiation of osteoblastic cells grown on the surface of a poly-L-lactide substrate. Med Biol Eng Comput. 2010; 48: 793-8.

39. Chuo W, Ma T, Saito T, Sugita Y, Maeda H, Zhang G, et al. A preliminary study of the effect of static magnetic field acting on rat bone marrow mesenchymal stem cells during osteogenic differentiation in vitro. J Hard Tissue Biology. 2013; 22: 227-32.

40. Rosen AD. Mechanism of action of moderate-intensity static magnetic fields on biological systems. Cell Biochem Biophys. 2003; 39: 163-73.

41. Kotani H, Iwasaka M, Ueno S. Magnetic orientation of collagen and bone mixture. J Appl Phys. 2000; 87: 6191-3.

42. Puricelli E, Ulbrich LM, Ponzoni D, Filho JJ. Histological analysis of the effects of a static magnetic field on bone healing process in rat femurs. Head Face Med. 2006; 2: 43.

43. Xu S, Tomita N, Ohata R, Yan Q, Ikada Y. Static magnetic field effects on bone formation of rats with an ischemic bone model. Biomed Mater Eng. 2001; 11: 257-63.

44. Taniguchi N, Kanai S, Kawamoto M, Endo H, Higashino H. Study on application of static magnetic field for adjuvant arthritis rats. Evid Based Complement Alternat Med. 2004; 1:

187-91.

45. Xu S, Okano H, Tomita N, Ikada Y. Recovery effects of a 180 mT static magnetic field on bone mineral density of osteoporotic lumbar vertebrae in ovariectomized rats. Evid Based Complement Alternat Med. 2011; 2011.

46. Puricelli E, Dutra NB, Ponzoni D. Histological evaluation of the influence of magnetic field application in autogenous bone grafts in rats. Head Face Med. 2009; 5: 1.

47. Markov MS. Therapeutic application of static magnetic fields. Environmentalist. 2007; 27: 457-63.

48. Miyakoshi J. Effects of static magnetic fields at the cellular level. Prog Biophys Mol Biol. 2005; 87: 213-23.

49. Marędziak M, Śmieszek A, Tomaszewski K A, Lewandowski D, Marycz K. The effect of low static magnetic field on osteogenic and adipogenic differentiation potential of human adipose stromal/stem cells. J Magnetism and Magnetic Materials. 2016; 398: 235-45.

50. Lew WZ, Huang YC, Huang KY, Lin CT, Tsai MT, Huang HM. Static magnetic fields enhance dental pulp stem cell proliferation by activating the p38 mitogen-activated protein kinase pathway as its putative mechanism. J Tissue Eng Regen Med. 2018; 12: 19-29.

51. Bassett CAL. Fundamental and practical aspects of therapeutic uses of pulsed electromagnetic fields (PEMFs). Crit Rev Biomed Eng. 1989; 17: 451-529.

52. Jing D, Zhai M, Tong S, Xu F, Cai J, Shen G, et al. Pulsed electromagnetic fields promote osteogenesis and osseointegration of porous titanium implants in bone defect repair through a Wnt/β-catenin signaling-associated mechanism. Sci Rep. 2016; 6: 32045.

53. Jing D, Cai J, Wu Y, Shen G, Li F, Xu Q, et al. Pulsed electromagnetic fields partially

preserve bone mass, microarchitecture, and strength by promoting bone formation in hindlimb-suspended rats. J Bone Miner Res. 2014; 29: 2250-61.

54. Lim K, Hexiu J, Kim J, Seonwoo H, Cho WJ, Choung PH, et al. Effects of electromagnetic fields on osteogenesis of human alveolar bone-derived mesenchymal stem cells. BioMed research international. 2013; 2013.

55. Yan JL, Zhou J, Ma HP, Ma XN, Gao YH, Shi WG, et al. Pulsed electromagnetic fields promote osteoblast mineralization and maturation needing the existence of primary cilia. Mol Cell Endocrinol. 2015; 404: 132-40.

56. Zhou J, He H, Yang L, Chen S, Guo H, Xia L, et al. Effects of pulsed electromagnetic fields on bone mass and Wnt/β-catenin signaling pathway in ovariectomized rats. Arch Med Res. 2012; 43: 274-82.

57. Kotani H, Kawaguchi H, Shimoaka T, Iwasaka M, Ueno S, Ozawa H, et al. Strong static magnetic field stimulates bone formation to a definite orientation in vitro and in vivo. J Bone Miner Res. 2002;17: 1814-21.

58. Li JK, Lin JC, Liu HC, Sun JS, Ruaan RC, Shih C, et al. Comparison of ultrasound and electromagnetic field effects on osteoblast growth. Ultrasound Med Biol. 2006; 32: 769-75.

59. Yong Y, Ming ZD, Feng L, Chun ZW, Hua W. Electromagnetic fields promote osteogenesis of rat mesenchymal stem cells through the PKA and ERK1/2 pathways. J Tissue Eng Regen Med. 2016; 10: E537-45.

60. He J, Zhang Y, Chen J, Zheng S, Huang H, Dong X. Effects of pulsed electromagnetic fields on the expression of NFATc1 and CAII in mouse osteoclast-like cells. Aging Clin Exp Res. 2015; 27: 13-9.

61. Jing D, Li F, Jiang M, Cai J, Wu Y, Xie K, et al. Pulsed electromagnetic fields improve bone microstructure and strength in ovariectomized rats through a Wnt/Lrp5/β-catenin signaling-associated mechanism. PLoS One. 2013; 8: e79377.

62. Ledda M, D'Emilia E, Giuliani L, Marchese R, Foletti A, Grimaldi S, et al. Nonpulsed sinusoidal electromagnetic fields as a noninvasive strategy in bone repair: the effect on human mesenchymal stem cell osteogenic differentiation. Tissue Eng Part C Methods. 2015; 21: 207-17.

63. Hu J, Zhang T, Xu D, Qu J, Qin L, Zhou J, et al. Combined magnetic fields accelerate bone-tendon junction injury healing through osteogenesis. Scand J Med Sci Sports. 2015; 25: 398-405.

64. Karthick T, Sengottuvelu S, Haja Sherief S, Duraisami. A Review: Biological effects of magnetic fields on rodents. Sch J App Med Sci. 2017; 5: 1569-80.

65. Gujjalapudi M, Anam C, Mamidi P, Chiluka R, Kumar AG, Bibinagar R. Effect of Magnetic Field on Bone Healing around Endosseous Implants–An In-vivo Study. Journal of clinical and diagnostic research: JCDR. 2016; 10: ZF01.

66. Yang J, Zhang J, Ding C, Dong D, Shang P. Regulation of Osteoblast Differentiation and Iron Content in MC3T3-E1 Cells by Static Magnetic Field with Different Intensities. Biol Trace Elem Res. 2018; 184: 214-25.

67. Markov MS. “Biological windows”: a tribute to W. Ross Adey. Environmentalist. 2005; 25: 67-74.

68. Kim EC, Park J, Kwon IK, Lee SW, Park SJ, Ahn SJ. Static magnetic fields promote osteoblastic/cementoblastic differentiation in osteoblasts, cementoblasts, and periodontal

ligament cells. J Periodontal Implant Sci. 2017; 47: 273-91.

69. Zhang J, Meng X, Ding C, Shang P. Effects of static magnetic fields on bone microstructure and mechanical properties in mice. Electromagn Biol Med. 2018; 37: 76-83.

70. Abreu MC, Ponzoni D, Langie R, Artuzi FE, Puricelli E. Effects of a buried magnetic field on cranial bone reconstruction in rats. J Appl Oral Sci. 2016; 24: 162-70.

71. Muramatsu Y, Matsui T, Deie M, Sato K. Pulsed Electromagnetic Field Stimulation Promotes Anti-cell Proliferative Activity in Doxorubicin-treated Mouse Osteosarcoma Cells. In Vivo. 2017; 31:61-8.

72. Arjmand M, Ardeshirylajimi A, Maghsoudi H, Azadian E. Osteogenic differentiation potential of mesenchymal stem cells cultured on nanofibrous scaffold improved in the presence of pulsed electromagnetic field. J Cell Physiol. 2018; 233: 1061-70.

73. Zhou J, Ma XN, Gao YH, Yan JL, Shi WG, Xian CJ, Chen KM. Sinusoidal electromagnetic fields promote bone formation and inhibit bone resorption in rat femoral tissues in vitro. Electromagn Biol Med. 2016; 35: 75-83.

74. Manjhi J, Kumar S, Behari J, Mathur R. Effect of extremely low frequency magnetic field in prevention of spinal cord injury-induced osteoporosis. J Rehabil Res Dev. 2013; 50: 17-30.

75. Xiong F, Wang H, Feng Y, Li Y, Hua X, Pang X, et al. Cardioprotective activity of iron oxide nanoparticles. Sci Rep. 2015; 5: 8579.

76. Henstock JR, Rotherham M, Rashidi H, Shakesheff KM, El Haj AJ. Remotely activated mechanotransduction via magnetic nanoparticles promotes mineralization synergistically with bone morphogenetic protein 2: Applications for injectable cell therapy. Stem Cells Transl Med. 2014; 3: 1363-74.

77. Wang Q, Chen B, Cao M, Sun J, Wu H, Zhao P, et al. Response of MAPK pathway to iron oxide nanoparticles in vitro treatment promotes osteogenic differentiation of hBMSCs. Biomaterials. 2016; 86: 11-20.

78. Hu S, Zhou Y, Zhao Y, Xu Y, Zhang F, Gu N, et al. Enhanced bone regeneration and

visual monitoring via super-paramagnetic iron oxide nanoparticle-scaffold in rats. J Tissue Eng Regen Med. J Tissue Eng Regen Med. 2018; 12: e2085-98.

79. Huang DM, Hsiao JK, Chen YC, Chien LY, Yao M, Chen YK, et al. The promotion of human mesenchymal stem cell proliferation by superparamagnetic iron oxide nanoparticles. Biomaterials. 2009; 30: 3645-51.

80. Wang Q, Chen B, Ma F, Lin S, Cao M, Li Y, et al. Magnetic iron oxide nanoparticles accelerate osteogenic differentiation of mesenchymal stem cells via modulation of long noncoding RNA INZEB2. Nano Research. 2017;10: 626-42.

81. Tschulik K, Compton RG. Nanoparticle impacts reveal magnetic field induced agglomeration and reduced dissolution rates. Phys Chem Chem Phys. 2014; 16: 13909-13.

82. Shanehsazzadeh S, Lahooti A, Hajipour MJ, Ghavami M, Azhdarzadeh M. External magnetic fields affect the biological impacts of superparamagnetic iron nanoparticles. Colloids Surf B Biointerfaces. 2015; 136: 1107-12.

83. Jiang P, Zhang Y, Zhu C, Zhang W, Mao Z, Gao C. Fe_3O_4/BSA particles induce osteogenic differentiation of mesenchymal stem cells under static magnetic field. Acta Biomater. 2016; 46: 141-50.

84. Panseri S, Cunha C, D'Alessandro T, Sandri M, Giavaresi G, Marcacci M, et al. Intrinsically superparamagnetic Fe-hydroxyapatite nanoparticles positively influence osteoblast-like cell behaviour. J Nanobiotechnology. 2012; 10: 32.

85. Qi Y, Feng G, Huang Z, Yan W. The application of super paramagnetic iron oxide-labeled mesenchymal stem cells in cell-based therapy. Mol Biol Rep. 2013; 40: 2733-40.

86. Andreas K, Georgieva R, Ladwig M, Mueller S, Notter M, Sittinger M, et al. Highly

efficient magnetic stem cell labeling with citrate-coated superparamagnetic iron oxide nanoparticles for MRI tracking. Biomaterials. 2012; 33: 4515-25.

87. Panseri S, Montesi M, Iafisco M, Adamiano A, Ghetti M, Cenacchi G, et al. Magnetic labelling of mesenchymal stem cells with iron-doped hydroxyapatite nanoparticles as tool for cell therapy. J Biomed Nanotechnol. 2016; 12: 909-21.

88. Wang Y, Wang Y, Wang L, Che Y, Li Z, Kong D. Preparation and evaluation of magnetic nanoparticles for cell labeling. J Nanosci Nanotechnol. 2011; 11: 3749-56.

89. Hill JM, Dick AJ, Raman VK, Thompson RB, Yu ZX, Hinds KA, et al. Serial cardiac magnetic resonance imaging of injected mesenchymal stem cells. Circulation. 2003; 108: 1009-14.

90. Saldanha KJ, Doan RP, Ainslie KM, Desai TA, Majumdar S. Micrometer-sized iron oxide particle labeling of mesenchymal stem cells for magnetic resonance imaging-based monitoring of cartilage tissue engineering. Magn Reson Imaging. 2011; 29: 40-9.

91. Thu MS, Bryant LH, Coppola T, Jordan EK, Budde MD, Lewis BK, et al. Self-assembling nanocomplexes by combining ferumoxytol, heparin and protamine for cell tracking by magnetic resonance imaging. Nat Med. 2012; 18: 463-7.

92. Lam T, Pouliot P, Avti PK, Lesage F, Kakkar AK. Superparamagnetic iron oxide based nanoprobes for imaging and theranostics. Adv Colloid Interface Sci. 2013; 199-200: 95-113.

93. Vogt C, Toprak MS, Muhammed M, Laurent S, Bridot JL, Muller RN. High quality and tuneable silica shell-magnetic core nanoparticles. J Nanoparticle Res. 2010; 12: 1137-47.

94. Chen F, Bu W, Lu C, Chen G, Chen M, Shen X, et al. Hydrothermal synthesis of a highly sensitive T2-weigthed MRI contrast agent: zinc-doped superparamagnetic iron oxide

nanocrystals. J Nanosci Nanotechnol. 2011; 11: 10438-43.

95. Fang QL, Xuan SH, Jiang WQ, Gong XL. Fang Q, Xuan S, et al. Yolk-like micro/nanoparticles with superparamagnetic iron oxide cores and hierarchical nickel silicate shell. Adv Funct Mater. 2011; 21: 1902-9.

96. Zhang Y, Wang SN, Ma S, Guan JJ, Li D, Zhang XD, et al. Self-assembly multifunctional nanocomposites with Fe_3O_4 magnetic core and CdSe/ZnS quantum dots shell. J Biomed Mater Res A. 2008; 85: 840-6.

97. Ren LL, Huang S, Fan W, Liu TX. One-step preparation of hierarchical superparamagnetic iron oxide/graphene composites via hydrothermal method. Appl Surf Sci. 2011; 258: 1132-8.

98. Chen B, Li Y, Zhang X, Liu F, Liu Y, Xiong F, et al. An efficient synthesis of ferumoxytol induced by alternating-current magnetic field. Materials Letters. 2016; 170: 93-6.

99. Maggio ND, Martella E, Meikle S, Columbaro M, Lucarelli E, Santin M, et al. Rapid and efficient magnetization of mesenchymal stem cells by dendrimer-functionalized magnetic nanoparticles. Nanomedicine (Lond). 2016; 11: 1519-34.

100. Arsalani N, Fattahi H, Laurent S, Burtea C, Vander Elst L, Muller RN. Polyglycerol-grafted superparamagnetic iron oxide nanoparticles: highly efficient MRI contrast agent for liver and kidney imaging and potential scaffold for cellular and molecular imaging. Contrast Media Mol Imaging. 2012; 7: 185-94.

101. Liu XL, Fan HM, Yi JB, Yang Y, Choo ESG, Xue JM, et al. Optimization of surface coating on Fe_3O_4 nanoparticles for high performance magnetic hyperthermia agents. J Mater Chem. 2012; 22: 8235-44.

102. He X, Wu X, Cai X, Lin S, Xie M, Zhu X, et al. Functionalization of magnetic nanoparticles with dendritic-linear-brush-like triblock copolymers and their drug release properties. Langmuir. 2012; 28: 11929-38.

103. Chang Y, Liu N, Chen L, Meng X, Liu Y, Li Y, et al. Synthesis and characterization of DOX-conjugated dendrimer-modified magnetic iron oxide conjugates for magnetic resonance imaging, targeting, and drug delivery. J Mater Chem. 2012; 22: 9594.

104. Zhou L, He B, Zhang F. Facile one-pot synthesis of iron oxide nanoparticles cross-linked magnetic poly(vinyl alcohol) gel beads for drug delivery. ACS Appl Mater Interfaces. 2012; 4: 192-9.

105. Josephson L, Tung CH, Moore A, Weissleder R. High-efficiency intracellular magnetic labeling with novel superparamagnetic-Tat peptide conjugates. Bioconjug Chem. 1999; 10: 186-91.

106. Lewin M, Carlesso N, Tung CH, Tang XW, Cory D, Scadden DT, et al. Tat peptide-derivatized magnetic nanoparticles allow in vivo tracking and recovery of progenitor cells. Nat Biotechnol. 2000; 18: 410-4.

107. Nitin N, LaConte LE, Zurkiya O, Hu X, Bao G. Functionalization and peptide-based delivery of magnetic nanoparticles as an intracellular MRI contrast agent. J Biol Inorg Chem. 2004; 9: 706-12.

108. Ichikawa T, Högemann D, Saeki Y, Tyminski E, Terada K, Weissleder R, et al. MRI of transgene expression: correlation to therapeutic gene expression. Neoplasia. 2002; 4: 523-30.

109. Jaffer FA, Weissleder R. Seeing within: molecular imaging of the cardiovascular system. Circ Res. 2004; 94: 433-45.

110. Kang HW, Josephson L, Petrovsky A, Weissleder R, Bogdanov A Jr. Magnetic resonance imaging of inducible E-selectin expression in human endothelial cell culture. Bioconjug Chem. 2002; 13: 122-7.

111. Lee DE, Kim AY, Saravanakumar G, Koo H, Kwon IC, Choi K, et al. Hyaluronidase-sensitive SPIONs for MR/optical dual imaging nanoprobes. Macromol Res 2011; 19: 861-7.

112. Meng Y, Shi C, Hu B, Gong J, Zhong X, Lin X, et al. External magnetic field promotes homing of magnetized stem cells following subcutaneous injection. BMC Cell Biol. 2017; 18: 24.

113. Sasaki H, Tanaka N, Nakanishi K, Nishida K, Hamasaki T, Yamada K, et al. Therapeutic effects with magnetic targeting of bone marrow stromal cells in a rat spinal cord injury model. Spine (Phila Pa 1976). 2011; 36: 933-8.

114. Mahmoud EE, Kamei G, Harada Y, Shimizu R, Kamei N, Adachi N, et al. Cell magnetic targeting system for repair of severe chronic osteochondral defect in a rabbit model. Cell Transplant. 2016; 25: 1073-83.

115. Kanczler JM, Sura HS, Magnay J, Green D, Oreffo RO, Dobson JP, et al. Controlled differentiation of human bone marrow stromal cells using magnetic nanoparticle technology. Tissue Eng Part A. 2010; 16: 3241-50.

116. Yang J, Yamato M, Shimizu T, Sekine H, Ohashi K, Kanzaki M, et al. Reconstruction of functional tissues with cell sheet engineering. Biomaterials. 2007; 28: 5033-43.

117. Kelm JM, Fussenegger M. Scaffold-free cell delivery for use in regenerative medicine. Adv Drug Deliv Rev. 2010; 62: 753-64.

118. Guillotin B, Guillemot F. Cell patterning technologies for organotypic tissue fabrication. Trends Biotechnol. 2011; 29: 183-90.

119. Pan Y, Du X, Zhao F, Xu B. Magnetic nanoparticles for the manipulation of proteins and cells. Chem Soc Rev. 2012; 41: 2912-42.

120. Frasca G, Gazeau F, Wilhelm C. Formation of a three-dimensional multicellular assembly using magnetic patterning. Langmuir. 2009; 25: 2348-54.

121. Zhang W, Yang G, Wang X, Jiang L, Jiang F, Li G, et al. Magnetically controlled growth-factor-immobilized multilayer cell sheets for complex tissue regeneration. Adv Mater. 2017; 29.

122. Bock N, Riminucci A, Dionigi C, Russo A, Tampieri A, Landi E, et al. A novel route in bone tissue engineering: magnetic biomimetic scaffolds. Acta Biomater. 2010; 6: 786-96.

123. Zeng XB, Hu H, Xie LQ, Lan F, Jiang W, Wu Y, et al. Magnetic responsive hydroxyapatite composite scaffolds construction for bone defect reparation. Int J Nanomedicine. 2012; 7: 3365-78.

124. Bianchi M, Boi M, Sartori M, Giavaresi G, Lopomo N, Fini M, et al. Nanomechanical mapping of bone tissue regenerated by magnetic scaffolds. J Mater Sci Mater Med. 2015; 26: 5363.

125. Samal SK, Dash M, Shelyakova T, Declercq HA, Uhlarz M, Bañobre-López M, et al. Biomimetic magnetic silk scaffolds. ACS Appl Mater Interfaces. 2015; 7: 6282-92.

126. Meng J, Zhang Y, Qi X, Kong H, Wang C, Xu Z, et al. Paramagnetic nanofibrous composite films enhance the osteogenic responses of pre-osteoblast cells. Nanoscale. 2010; 2: 2565-9.

127. Cai Q, Shi Y, Shan D, Jia W, Duan S, Deng X, et al. Osteogenic differentiation of MC3T3-E1 cells on poly(l-lactide)/Fe3O4 nanofibers with static magnetic field exposure. Mater Sci Eng C Mater Biol Appl. 2015; 55: 166-73.

128. Wei Y, Zhang X, Song Y, Han B, Hu X, Wang X, et al. Magnetic biodegradable Fe_3O_4/CS/PVA nanofibrous membranes for bone regeneration. Biomed Mater. 2011; 6:055008.

129. Mortimer CJ, Wright CJ. The fabrication of iron oxide nanoparticle-nanofiber composites by electrospinning and their applications in tissue engineering. Biotechnol J. 2017; 12

130. Daňková J, Buzgo M, Vejpravová J, Kubíčková S, Sovková V, Vysloužilová L, et al. Highly efficient mesenchymal stem cell proliferation on poly-ε-caprolactone nanofibers with embedded magnetic nanoparticles. Int J Nanomedicine. 2015; 10: 7307-17.

131. Russo A, Bianchi M, Sartori M, Boi M, Giavaresi G, Salter DM, et al. Bone regeneration in a rabbit critical femoral defect by means of magnetic hydroxyapatite macroporous scaffolds. J Biomed Mater Res B Appl Biomater. 2018; 106: 546-54.

132. De Santis R, Russo A, Gloria A, D'Amora U, Russo T, Panseri S, et al. Towards the Design of 3D Fiber-Deposited Poly(ε-caprolactone)/Iron-Doped Hydroxyapatite Nanocomposite Magnetic Scaffolds for Bone Regeneration. J Biomed Nanotechnol. 2015; 11: 1236-46.

133. Zhang JH, Zhao SC, Zhu M, Zhu YF, Zhang YD, Liu ZT, et al. 3D-printed magnetic Fe_3O_4/MBG/PCL composite scaffolds with multifunctionality of bone regeneration, local anticancer drug delivery and hyperthermia. J Mater Chem B. 2014; 2: 7583-95.

134. Tampieri A, Landi E, Valentini F, Sandri M, D'Alessandro T, Dediu V, et al. A conceptually new type of bio-hybrid scaffold for bone regeneration. Nanotechnology. 2011; 22: 015104.

135. Wang H, Zhao SC, Zhou J, Zhu KP, Cui X, Huang WH, et al. Biocompatibility and osteogenic capacity of borosilicate bioactive glass scaffolds loaded with Fe_3O_4 magnetic nanoparticles. J Mater Chem B. 2015; 3: 4377-87.

136. Xia Y, Chen H, Zhang F, Wang L, Chen B, Reynolds MA, et al. Injectable calcium phosphate scaffold with iron oxide nanoparticles to enhance osteogenesis via dental pulp stem cells. Artif Cells Nanomed Biotechnol. 2018: 1-11.

137. Perez RA, Patel KD, Kim HW. Novel magnetic nanocomposite injectables: Calcium phosphate cements impregnated with ultrafine magnetic nanoparticles for bone regeneration. RSC Advances. 2015; 5:13411-9.

138. Dashnyam K, Perez RA, Singh RK, Lee EJ, Kim HW. Hybrid magnetic scaffolds of gelatin-siloxane incorporated with magnetite nanoparticles effective for bone tissue engineering. RSC Adv. 2014;4: 40841-51.

139. Díaz E, Valle MB, Barandiarán JM. Magnetic composite scaffolds of polycaprolactone/nFeHA, for bone-tissue engineering. Inter J Polymeric Mater Polymeric Biomater. 2016; 65: 593-600.

140. Zhu YF, Shang FJ, Li B, Dong Y, Liu YF, Lohe MR, et al. Magnetic mesoporous bioactive glass scaffolds: preparation, physicochemistry and biological properties. J Mater Chem. B. 2013; 1:1279-88.

141. Wu C, Fan W, Zhu Y, Gelinsky M, Chang J, Cuniberti G, et al. Multifunctional magnetic

mesoporous bioactive glass scaffolds with a hierarchical pore structure. Acta Biomater. 2011; 7: 3563-72.

142. Zhu M, Zhang JH, Zhou YH, Liu YF, He X, Tao CL, et al. Preparation and characterization of magnetic mesoporous bioactive glass/carbon composite scaffolds. J Chem. 2013; 893479.

143. Gloria A, Russo T, D'Amora U, Zeppetelli S, D'Alessandro T, Sandri M, et al. Magnetic poly(ε-caprolactone)/iron-doped hydroxyapatite nanocomposite substrates for advanced bone tissue engineering. J R Soc Interface. 2013; 10: 20120833.

144. Richardson JJ, Björnmalm M, Caruso F. Multilayer assembly. Technology-driven layer-by-layer assembly of nanofilms. Science. 2015; 348: aaa2491.

145. Tang Y, Zhao Y, Wang X, Lin T. Layer-by-layer assembly of silica nanoparticles on 3D fibrous scaffolds: enhancement of osteoblast cell adhesion, proliferation, and differentiation. J Biomed Mater Res A. 2014; 102: 3803-12.

146. Chen HM, Sun JF, Wang ZB, Zhou Y, Lou ZC, Chen B, et al. Magnetism-enhanced osteogenic differentiation of adipose-derived stem cells by magnetic cell-scaffold interface. ACS Appl Mater Interfaces. Revised.

147. Yang D, Lu B, Zhao Y, Jiang X. Fabrication of aligned fibrous arrays by magnetic electrospinning. Adv Mater. 2007; 19: 3702-6.

148. Lee WY, Cheng WY, Yeh YC, Lai CH, Hwang SM, Hsiao CW, et al. Magnetically directed self-assembly of electrospun superparamagnetic fibrous bundles to form three-dimensional tissues with a highly ordered architecture. Tissue Eng Part C Methods. 2011; 17: 651-61.

149. Li Q, Ge L, Wan W, Jiang J, Zhong W, Ouyang J, et al. Magnetically guided fabrication of multilayered iron oxide/polycaprolactone/gelatin nanofibrous structures for tissue engineering and theranostic application. Tissue Eng Part C Methods. 2015; 21: 1015-24.

150. Frank MB, Naleway SE, Haroush T, Liu CH, Siu SH, Ng J, et al. Stiff, porous scaffolds from magnetized alumina particles aligned by magnetic freeze casting. Mater Sci Eng C Mater Biol Appl. 2017; 77: 484-92.

151. Frank MB, Hei Siu S, Karandikar K, Liu CH, Naleway SE, Porter MM, et al. Synergistic structures from magnetic freeze casting with surface magnetized alumina particles and platelets. J Mech Behav Biomed Mater. 2017; 76: 153-63.

152. Infanger DW, Lynch ME, Fischbach C. Engineered culture models for studies of tumor-microenvironment interactions. Annu Rev Biomed Eng. 2013; 15: 29-53.

153. Ganesh N, Ashokan A, Rajeshkannan R, Chennazhi K, Koyakutty M, Nair SV. Magnetic resonance functional nano-hydroxyapatite incorporated poly(caprolactone) composite scaffolds for in situ monitoring of bone tissue regeneration by MRI. Tissue Eng Part A. 2014; 20: 2783-94.

154. Yun HM, Lee ES, Kim MJ, Kim JJ, Lee JH, Lee HH, et al. Magnetic Nanocomposite Scaffold-Induced Stimulation of Migration and Odontogenesis of Human Dental Pulp Cells through Integrin Signaling Pathways. PLoS One. 2015;10: e0138614.

155. Arjmand M, Ardeshirylajimi A, Maghsoudi H, Azadian E. Osteogenic differentiation potential of mesenchymal stem cells cultured on nanofibrous scaffold improved in the presence of pulsed electromagnetic field. J Cell Physiol. 2018; 233: 1061-70.

156. Meng J, Xiao B, Zhang Y, Liu J, Xue H, Lei J, et al. Super-paramagnetic responsive

nanofibrous scaffolds under static magnetic field enhance osteogenesis for bone repair in vivo. Sci Rep. 2013; 3: 2655.

157. Yun HM, Ahn SJ, Park KR, Kim MJ, Kim JJ, Jin GZ, et al. Magnetic nanocomposite scaffolds combined with static magnetic field in the stimulation of osteoblastic differentiation and bone formation. Biomaterials. 2016; 85: 88-98.

158. Shimizu K, Ito A, Honda H. Enhanced cell-seeding into 3D porous scaffolds by use of magnetite nanoparticles. J Biomed Mater Res B Appl Biomater. 2006; 77: 265-72.

159. Thevenot P, Sohaebuddin S, Poudyal N, Liu JP, Tang L. Magnetic nanoparticles to enhance cell seeding and distribution in tissue engineering scaffolds. Proc IEEE Conf Nanotechnol. 2008; 2008: 646-9.

160. Shimizu K, Ito A, Honda H. Mag-seeding of rat bone marrow stromal cells into porous hydroxyapatite scaffolds for bone tissue engineering. J Biosci Bioeng. 2007; 104: 171-7.

161. Russo A, Bianchi M, Sartori M, Parrilli A, Panseri S, Ortolani A, et al. Magnetic forces and magnetized biomaterials provide dynamic flux information during bone regeneration. J Mater Sci Mater Med. 2016; 27: 51.

162. Paun IA, Popescu RC, Calin BS, Mustaciosu CC, Dinescu M, Luculescu CR. 3D Biomimetic Magnetic Structures for Static Magnetic Field Stimulation of Osteogenesis. Int J Mol Sci. 2018;19: E495.

163. Tampieri A, Iafisco M, Sandri M, Panseri S, Cunha C, Sprio S, et al. Magnetic bioinspired hybrid nanostructured collagen-hydroxyapatite scaffolds supporting cell proliferation and tuning regenerative process. ACS Appl Mater Interfaces. 2014; 6: 15697-707.

164. Huang J, Wang D, Chen J, Liu W, Duan L, You W, et al. Osteogenic differentiation of bone marrow mesenchymal stem cells by magnetic nanoparticle composite scaffolds under a pulsed electromagnetic field. Saudi Pharm J. 2017; 25: 575-9.

165. Ho-Shui-Ling A, Bolander J, Rustom LE, Johnson AW, Luyten FP, Picart C. Bone regeneration strategies: Engineered scaffolds, bioactive molecules and stem cells current stage and future perspectives. Biomaterials. 2018; 180: 143-62.

166. Levy I, Sher I, Corem-Salkmon E, Ziv-Polat O, Meir A, Treves AJ, et al. Bioactive magnetic near Infra-Red fluorescent core-shell iron oxide/human serum albumin nanoparticles for controlled release of growth factors for augmentation of human mesenchymal stem cell growth and differentiation. J Nanobiotechnology. 2015; 13: 34.

167. Silva ED, Babo PS, Costa-Almeida R, Domingues RMA, Mendes BB, Paz E, et al. Multifunctional magnetic-responsive hydrogels to engineer tendon-to-bone interface. Nanomedicine. 2017. pii: S1549-9634(17)30108-9.

168. Wang L, Jang G, Ban DK, Sant V, Seth J, Kazmi S, et al. Multifunctional stimuli responsive polymer-gated iron and gold-embedded silica nano golf balls: Nanoshuttles for targeted on-demand theranostics. Bone Res. 2017; 5: 17051.

169. Novickij V, Stanevičienė R, Vepštaitė-Monstavičė I, Gruškienė R, Krivorotova T, Sereikaitė J, et al. Overcoming antimicrobial resistance in bacteria using bioactive magnetic nanoparticles and pulsed electromagnetic fields. Front Microbiol. 2018; 8: 2678.

170. Dobretsov K, Stolyar S, Lopatin A. Magnetic nanoparticles: a new tool for antibiotic delivery to sinonasal tissues. Results of preliminary studies. Acta Otorhinolaryngol Ital. 2015; 35: 97-102.

171. Skaat H, Ziv-Polat O, Shahar A, Last D, Mardor Y, Margel S. Magnetic scaffolds enriched with bioactive nanoparticles for tissue engineering. Adv Healthc Mater. 2012; 1: 168-71.

172. Angrisani N, Foth F, Kietzmann M, Schumacher S, Angrisani GL, Christel A, et al. Increased accumulation of magnetic nanoparticles by magnetizable implant materials for the treatment of implant-associated complications. J Nanobiotechnology. 2013; 11: 34.

173. Rotherham M, El Haj AJ. Remote activation of the Wnt/β-catenin signalling pathway using functionalised magnetic particles. PLoS One. 2015; 10: e0121761.

174. Hu B, El Haj AJ, Dobson J. Receptor-targeted, magneto-mechanical stimulation of osteogenic differentiation of human bone marrow-derived mesenchymal stem cells. Int J Mol Sci. 2013; 14: 19276-93.

175. Rotherham M, Henstock JR, Qutachi O, El Haj AJ. Remote regulation of magnetic particle targeted Wnt signaling for bone tissue engineering. Nanomedicine. 2018; 14: 173-84.

176. Minear S, Leucht P, Jiang J, Liu B, Zeng A, Fuerer C, et al. Wnt proteins promote bone regeneration. Sci Transl Med. 2010; 2: 29ra30.

177. Sapet C, Pellegrino C, Laurent N, Sicard F, Zelphati O. Magnetic nanoparticles enhance adenovirus transduction in vitro and in vivo. Pharm Res. 2012; 29: 1203-18.

178. Zhou Y, Tang Z, Shi C, Shi S, Qian Z, Zhou S. Polyethylenimine functionalized magnetic nanoparticles as a potential non-viral vector for gene delivery. J Mater Sci Mater Med. 2012; 23: 2697-708.

179. Rodrigues AR, Gomes IT, Almeida BG, Araújo JP, Castanheira EM, Coutinho PJ. Magnetic liposomes based on nickel ferrite nanoparticles for biomedical applications. Phys

Chem Chem Phys. 2015; 17: 18011-21.

180. Zhang ZB, Song LN, Dong JL, Guo DW, Du XL, Cao BY, et al. A promising combo gene delivery system developed from (3-Aminopropyl) triethoxysilane-modified iron oxide nanoparticles and cationic polymers. J Nanopart Res. 2013; 15: 1659.

181. Zhang TY, Wu JH, Xu QH, Wang XR, Lu J, Hu Y, et al. Design of magnetic gene complexes as effective and serum resistant gene delivery systems for mesenchymal stem cells. Int J Pharm. 2017; 520: 1-13.

182. Gandra N, Wang DD, Zhu Y, Mao C. Virus-mimetic cytoplasm-cleavable magnetic/silica nanoclusters for enhanced gene delivery to mesenchymal stem cells. Angew Chem Int Ed Engl. 2013; 52: 11278-81.

183. McBain SC, Yiu HHP, El Haj A, Dobson J. Polyethyleneimine functionalized iron oxide nanoparticles as agents for DNA delivery and transfection. J Mater Chem. 2007; 17: 2561-5.

184. Podaru G, Ogden S, Baxter A, Shrestha T, Ren S, Thapa P, et al. Pulsed magnetic field induced fast drug release from magneto liposomes via ultrasound generation. J Phys Chem B. 2014; 118: 11715-22.

185. Peng Z, Fang E, Wang C, Lu X, Wang G, Tong Q. Construction of novel thermosensitive Magnetic cationic liposomes as a drug and gene co-delivery system. J Nanosci Nanotechnol. 2015; 15: 3823-33.

186. Nakayama Y, Mustapić M, Ebrahimian H, Wagner P, Kim JH, Hossain MS, et al. Magnetic nanoparticles for "smart liposomes". Eur Biophys J. 2015; 44: 647-54.

187. Pan X, Guan J, Yoo JW, Epstein AJ, Lee LJ, Lee RJ. Cationic lipid-coated magnetic nanoparticles associated with transferrin for gene delivery. Int J Pharm. 2008; 358: 263-70.

188. Liu Y, Yang F, Yuan C, Li M, Wang T, Chen B, et al. Magnetic nanoliposomes as in situ microbubble bombers for multimodality image-guided cancer theranostics. ACS Nano. 2017; 11: 1509-19.

189. Heymer A, Haddad D, Weber M, Gbureck U, Jakob PM, Eulert J, et al. Iron oxide labelling of human mesenchymal stem cells in collagen hydrogels for articular cartilage repair. Biomaterials. 2008; 29: 1473-83.

190. Hori J, Deie M, Kobayashi T, Yasunaga Y, Kawamata S, Ochi M. Articular cartilage repair using an intra-articular magnet and synovium-derived cells. J Orthop Res. 2011; 29: 531-8.

191. Markides H, Kehoe O, Morris RH, El Haj AJ. Whole body tracking of superparamagnetic iron oxide nanoparticle-labelled cells--a rheumatoid arthritis mouse model. Stem Cell Res Ther. 2013; 4: 126.

192. Lee JH, Jung MJ, Hwang YH, Lee YJ, Lee S, Lee DY, et al. Heparin-coated superparamagnetic iron oxide for in vivo MR imaging of human MSCs. Biomaterials. 2012; 33: 4861-71.

193. Chen JR. Noninvasive method for in vivo tracking of the regeneration of tissue engineering articular cartilage. Doctoral dissertations of Third Military Medical University. 2013.

194. Huang X, Zhang F, Wang Y, Sun X, Choi KY, Liu D, et al. Design considerations of iron-based nanoclusters for noninvasive tracking of mesenchymal stem cell homing. ACS Nano. 2014; 8: 4403-14. Erratum in: ACS Nano. 2014; 8: 7549.

195. Cho MH, Lee EJ, Son M, Lee JH, Yoo D, Kim JW, et al. magnetic switch for the control

of cell death signalling in in vitro and in vivo systems. Nat Mater. 2012; 11: 1038-43.

196. Jang JT, Nah H, Lee JH, Moon SH, Kim MG, Cheon J. Critical enhancements of MRI contrast and hyperthermic effects by dopant-controlled magnetic nanoparticles. Angew Chem Int Ed Engl. 2009; 48:1234-8.

197. Khan WS, Hardingham TE. The characterisation of mesenchymal stem cells: a stem cell is not a stem cell is not a stem cell. J Stem Cells. 2012; 7: 87-95.

198. Mertens ME, Hermann A, Bühren A, Olde-Damink L, Möckel D, Gremse F, et al. Iron oxide-labeled collagen scaffolds for non-invasive MR imaging in tissue engineering. Adv Funct Mater. 2014; 24: 754-62.

199. Rahmi G, Pidial L, Silva AK, Blondiaux E, Meresse B, Gazeau F, et al. Designing 3D mesenchymal stem cell sheets merging magnetic and fluorescent features: When cell sheet technology meets image-guided cell therapy. Theranostics. 2016; 6: 739-51.

200. Wartella KA, Khalilzad-Sharghi V, Kelso ML, Kovar JL, Kaplan DL, Xu H, et al. Multi-modal imaging for assessment of tissue-engineered bone in a critical-sized calvarial defect mouse model. J Tissue Eng Regen Med. 2017; 11: 1732-40.

201. Kłodowski K, Kamiński J, Nowicka K, Tarasiuk J, Wroński S, Swiętek M, et al. Micro-imaging of implanted scaffolds using combined MRI and micro-CT. Comput Med Imaging Graph. 2014; 38: 458-68.

Acknowledgments

This study was supported by National Institutes of Health R01 DE14190 and R21

DE22625, National Natural Science Foundation of China 81771044, National Key Research Project 2016YFA0201704/2016YFA0201700 and 2017YFA0104301, Jiangsu Medical Youth Talent QNRC2016853, Qing Lan Project, the Southeast University-Nanjing Medical University Cooperative Research Project 2242018K3DN16, Project Funded by the Priority Academic Program of Jiangsu Higher Education Institutions 2014-37, Collaborative Innovation Center of Suzhou Nano Science and Technology, and University of Maryland School of Dentistry bridge fund.

Figure captions

[1]. Effects of 4-week PEMF exposure on trabecular bone microarchitecture in the distal femora and cortical bone thickness in the mid-diaphysis of the femora, and the histology and histomorphometry in HU rats. (A) The selected volume of interest (VOI). (B) and (C) 3-D and 2-D MicroCT images of trabecular bone microarchitecture. Statistical comparisons of (D) trabecular BMD, (E) trabecular number (Tb.N), (F) trabecular thickness (Tb.Th), (G) BV/TV, (H) bone surface per bone volume (BS/BV), and (I) trabecular separation (Tb.Sp). Representative histological images for bone microarchitecture of the distal femora by Van Gieson staining, (J) Control; (K) HU; (L) HU+PEMF. Scale bar =1000 μm. (adapted from Ref. 53 with permission).

[2]. Detection of genes involved in classical MAPK signal pathway. (A) Expression of mRNAs detected by Q-PCR after 100 μg/mL SPIONs exposure 7 days. All bars represent mean ± SD, n=3, *** $p < 0.001$. (B) Expression of the total protein level and the phosphorylated protein form, detected by western blot analysis after 50 and 100 μg/mL

SPIONs exposure 7 days. (C) Schematic illustration of SPIONs-promoted osteogenic differentiation. (adapted from Ref. 68 with permission).

[3]. Manipulation of nGO@Fe_3O_4 MNP-labeled DPSCs via magnetic force. (A) The strategy for fabricating magnetically controlled cell sheets. (B) The magnet pattern controlled the shape of cell sheets. (C) Cell accumulation was observed at the marginal region of the cell sheet. (D) The marginal region of the cell sheet was observed after 24 h of culture. (E) A monkey-face-like cell-sheet pattern was fabricated via three hollow-cylinder magnets. The local region surrounded by the yellow rectangular frame is magnified and presented in (F). (G) Cells were arranged in regular continuous curves. (H) A merged image of cell distribution and the characteristic curves. (I) Schematic illustration of the fabrication strategy to form bilayer cell sheets. (J) The accumulation of GFP^+ cells on the RFP^+ cell sheet was observed under a fluorescence microscope. (K) The bilayer cell sheets were observed after 24 h of culture. (L) Schematic illustration of the two-step strategy to fabricate inlaid cell sheets. (M) The clear boundary line between GFP^+ cells and RFP^+ cells was observed. (N) The color of the cell sheets. (O) Representative HE staining image of nGO@ Fe_3O_4 MNP-labeled DPSC cell sheets. (P) Prussian-blue-stained paraffin sections of cell sheets. (Q) By adding cells repeatedly every 4 h, cell sheets with different thicknesses were obtained (n = 6) (★★, represents $p < 0.01$). (adapted from Ref. 112 with permission).

[4]. Magnetic CPC and its biological performance. (A) CPC control, γIONP-CPC and αIONP-CPC. Only γIONP-CPC was attracted by a magnet. (B) Cell spreading area on the scaffold. (C) Cell adhesion ratio normalized by culture well control (n = 4). The

mRNA expression levels of osteogenic genes in hDPSCs at 7 days and 14 days, with all data relative to hDPSCs on CPC control. Expression levels of ALP (D), COLI (E), RUNX2 (F), and OCN (G) (n = 3). In each plot, bars with different letters are significantly different ($p < 0.05$). (adapted from Ref. 136 with permission).

[5]. SEM images: ES Control (A); IO-ES (B); G-ES (C). (D) ALP activities of seeded cells at 4, 7, 14 days after seeding (n = 4). (E) (F) (G) and (H) The expressions of ALP, COL1, RUNX2, and OCN on the scaffolds after 7 days and 14 days culture (n = 4). (I) Quantitative analysis of mineral synthesis by the cells (n = 6). In each plot, bars indicated by different letters are significantly different from each other ($p < 0.05$). (adapted from Ref. 136 with permission).

[6]. The synergism of magnetic nanocomposite scaffolds combined with static magnetic field. (A) Characterization of the super-paramagnetic nanofibrous scaffolds. (B) Scheme image of the scaffold pellet being implanted in the defect of transverse process of L5 of rabbits. (C) SEM image of the scaffold showing randomly tangled nanofibers. (D) TEM image of fibers in the scaffold. (E) CT images of the bone defects for group S and Group S + M post 10, 50 and 90 days implantation. The arrows pointed to the defects. (F) Schematic illustration showing the combined magnetic cues from internal magnetic nanoparticles and the external magnetic field that can influence the cell responses. (G) Schematic diagram, illustrating the integrin, BMP, MAPK and NF-κB signaling pathways in osteoblasts synergized by the culture with SMF and magnetic scaffolds, which ultimately stimulating osteoblastic differentiation and bone regeneration. (adapted from Refs. 145 and 146 with permission).

[7]. Concepts and schematic of AMLs and their nano to micro conversion for ultrasound/MR dual modal imaging and the spatiotemporal bombed combination tumor accurate therapy. (adapted from Ref. 172 with permission).

[8]. MRI *in vivo*. T2-weighted MRI of incisor sockets at 0 day, 2 and 4 weeks after surgery, (a) Blank group, (b) GS group, (c) SPIONs-GS group; (d) Quantitative analyses of MRI *in vivo* according to grayscale changes. Significant differences between the three groups were detected at 0 day, and 2 and 4 weeks after surgery (mean ± sd; n = 9, $*p < 0.05$, $**p < 0.01$). (adapted from Ref. 69 with permission).

Table 1. Biological effects of different types, intensities and frequencies of magnetic fields for bone tissue engineering

Type	Intensities	Frequencies	Exposure method	Biological effects	Mechanisms
SMF [68]	15 mT	0 Hz	Continuous exposure	Enhanced osteogeneses of human osteoblasts, periodontal ligament cells, and cementoblasts (with bio-chemicals).	Activated Wnt/β-catenin, p38 and JNK, MAPK, and NF-κB signaling.
SMF [66]	500 nT, 0.2 T, 16 T	0Hz	Continuous exposure	500 nT and 0.2 T SMF exerted deleterious effects on MC3T3-E1 cells differentiation, while 16T SMF enhanced mineralization (with bio-chemicals).	16T increased transferrin receptor 1 and ferroportin 1.
SMF [10]	3mT, 15mT, 50mT	0Hz	Continuous exposure	Promoted proliferation and osteoblastic differentiation of hMSCs (with bio-chemicals).	Not detected.
SMF [65]	500 Guass	0Hz	12-15h/day for 90 days	Promoted bone healing around endosseous implants in humans.	Not detected.
SMF [69]	500nT, 200mT	0Hz	Continuous exposure for 4 weeks	Both SMFs did not have a significant effect on the bone microstructure and bone density of mice.	Ion metabolism might be involved.
SMF [32]	220–260 Gauss	0Hz	Continuous exposure for 4 weeks	Improved bone healing of New Zealand white rabbits in the first two weeks but had minor effects on bone mineral density values.	Not detected.
SMF [70]	84.3 Gauss	0Hz	Continuous exposure	SMF enhanced bone regeneration in rats.	Not detected.
PEMF [33]	2± 0.2 mT	75± 2 Hz	Pulse duration 1.3 ms, 10 min/day for 27 days	Promotes the osteogenesis of hMSC derived from bone marrow stroma (with bio-chemicals).	Enhanced expression of L-type voltage-gated Ca channels and modulation of the concentration of cytosolic free Ca^{2+}.

PEMF [71]	5 mT	200 Hz	1 and 12h	Enhanced the inhibition of cell proliferation mediated by doxorubicin but did not affect the cell cycle, mitochondrial membrane potential, or doxorubicin-induced G2/M arrest.	Enhanced doxorubicin-derived apoptosis.
PEMF [28]	16 Gauss	15Hz	8h/day for 3 days	Upregulated Intervertebral Disc-Cell Matrix Synthesis (with bio-chemicals).	Not detected.
PEMF [29]	1.8mT and 2.4mT	15 Hz	1h/day	No effect on the proliferation, but enhance the osteogenic differentiation of PDLSCs (with bio-chemicals).	Not detected.
PEMF [72]	1 mT	50 Hz	6h/day	Enhanced osteogenic differentiation of hADMSCs (with bio-chemicals).	Not detected.
SEMF [73]	1.8 mT	50 Hz	1.5h/day for 12 days	Promoted bone formation, increased metabolism and inhibited resorption in both metaphyseal and diaphyseal bone tissues in rat femoral tissues in vitro.	Not detected.
PEMF [30]	1.5mT	50Hz	Pulse duration 25 μs, 8h/day, 7^{th} day till 1 month	Enhanced bone regeneration in rats Zygomatic Bone Defect Model with platelet-rich plasma.	Not detected.
PEMF [61]	2.4 mT (peak value)	15 Hz	8h/day for 10 weeks	Improved bone mass and bone architecture, attenuated the biomechanical strength deterioration, in variectomized rats.	Promoted Wnt/LRP5/β-catenin signaling.
PEMF [53]	2.4 mT	15 Hz	2h/day for 4 weeks	Alleviated disuse-induced bone loss by promoting skeletal anabolic activities in hindlimb-unloaded rats.	Enhance Wnt/Lrp5/β-catenin signaling.
ELF-MF [74]	17.96 μT	50 Hz	2h/day, for 8 weeks	Attenuating spinal cord injury -induced osteoporosis in rats.	Not detected.
RMF [16]	0.32T and 0.6T	8–10 Hz	2h/day for 2 months	The osteogenesis regeneration of the necrotic femoral head was markedly improved in New Zealand rabbit	Not detected.

				models.	
Non-PSE MF [62]	1 mT	50 kHz	5 days	Enhanced osteoblast differentiation of hMSCs (with and without bio-chemicals).	Not detected.
AEF [17]	10 or 40 mA	10 Hz,	6 h/day for 14 days	Promoted the osteogenic differentiation of adult hMSCs (no bio-chemicals).	Not detected.
CMF [63]	400 mG	76.6 Hz	30 min/day, 3th day till 16 weeks	Promoted osteogenesis at the bone-tendon junction interface in a partial patellectomy rabbit mode.	Not detected.

Abbreviations: SMF: static magnetic field; PEMF: pulsed electromagnetic fields; hMSCs: human mesenchymal stem cells; RMF: rotating magnetic fields; AEF: alternating electromagnetic fields; PDLSCs: periodontal ligament stem cells; hADMSCs: human adipose-derived mesenchymal stem cells; SEMF: sinusoidal electromagnetic fields; ELF-MF: extremely low frequency magnetic field; Non-PSEMF: nonpulsed sinusoidal electromagnetic fields; CMF: combined magnetic field, a unique electromagnetic field that includes a dynamic sinusoidal magnetic field and a magnetostatic field.

Table 2. Magnetic scaffolds and their properties without using magnetic fields

Fabricating method	Matrix	MC/MI	Biological properties	Mechanisms
Dip-coating	HA and Col (70:30 w/w) [122]	15 emu/g at 10 kOe	Supported adhesion and proliferation of hBMSCs in vitro (with bio-chemicals).	Not mentioned.
	HA [123]	0.2-2.0 wt%	Positive influence of the magnetic scaffolds on ROS 17/2.8 and MC3T3-E1 cells adhesion, proliferation, and differentiation (no bio-chemicals).	The intrinsic nanoscale magnetic field provided by the incorporated MNPs.
	Silk fibroin protein scaffolds [125]	50μL/mL, 250μL/mL	Excellent hyperthermia properties, not toxic to MC3T3-E1 cells and improved cell adhesion and proliferation (with bio-chemicals).	Not mentioned.
	HA and Col [124]	15 emu/g at 10 kOe	Provided regenerated bone tissue with mechanical properties closer to that of native bone in male rabbits 4 weeks after surgery.	Different distribution of the magnetic nanoparticles inside the scaffold led to incongruous gradients of magnetic moment.
Co-electrospinning	Chitosan/ PVA [128]	5 wt%	Good cell adhesion and proliferation of MG63 cells (no bio-chemicals).	The micro-environments in the pores or on the surface of the scaffolds were composed of a great number of tiny magnetic fields.
	PCL [130]	10%wt	Great biocompatibility, ability to promote cellular adhesion, accelerate MSCs' proliferation, and support osteogenic differentiation (no bio-chemicals).	Magnetic scaffolds can generate a magnetic field to the surroundings, which consequently alters microenvironment conditions of cells.
	PCL [153]	MF-nHAp, 2.67% (w/w)	Biocompatible and promoted the proliferation of hMSCs. Improved the bioactivity of the scaffolds and supported early osteogenic differentiation of hMSCs.	The small concentration of 0.01 nM gadolinium doping. And hMSCs exposed to MF-nHAp within the PCL nanofibers.

Rapid prototyping technique	PCL [132]	FeHA, 80/20 w/w	In vitro, cell grew 2.2-fold greater. In vivo, PCL/FeHA scaffolds were completely filled with newly formed bone after only 4 weeks.	To reproduce a microenvironment that is both biologically and biomechanically adequate for bone regeneration.
	MBG/PCL [133]	5%, 10%, 15% wt	Endowed excellent magnetic heating ability and significantly stimulated osteogeneses of hBMSCs. (no bio-chemicals).	Ion channels on the cell membrane are affected by MNPs.
In situ nucleating	HA and Col (70:30 w/w) [134]	0.50 ±0.07 emu/g	Provided suitable microenvironments for supporting the adhesion, growth, and proliferation of hBMSCs.	Peculiar chemico-physical characteristics to the material.
Foam technique	HA [131]	90/10 wt	Induce and support bone tissue formation at both experimental time points without adverse tissue reactions in rabbits.	The intrinsic magnetic strength conferred by superparamagnetic nanoparticles on bone regeneration processes.
	Borosilicate bioactive glass [135]	5–15 wt%	Osteogenic differentiation of the hBMSCs was increased. 15 wt% MNPs scaffolds showed a significantly better capacity to regenerate bone in rat calvarial defects (no bio-chemicals).	Not mentioned.
Chemical reaction	CPC [136]	1% wt	Substantial increases in ALP activity, osteogenic gene expressions and bone matrix mineral synthesis (with bio-chemicals).	The surface nanotopography, and the cell internalization of IONPs released from IONP-CPC scaffold.
	CPC [137]	0-5% wt	The cells adhered and spread more actively. And enhanced cell proliferation and osteogenic differentiation (no bio-chemicals).	Decreased the crystal size of the HA altered surface morphology of the scaffold, and increased the surface area.
Freeze-drying	Gelatin–siloxane hybrids [138]	0-3% wt (0.24-0.64 emu/g)	Rat MSCs cultured on the scaffolds spread and proliferated better. Osteogenic differentiation was significantly higher (no bio-chemicals).	The existence of MNs at the subcellular level would influence the cellular reactions; the dissolution of iron ions from the MNs.
	PCL [139]	nFeHA 10-80% wt	Not detected.	Not detected.
	PCL [154]	5%, 10% wt	Provide excellent matrix conditions for hDPCs in their	Upregulated the integrin subunits and activated

			migration, adhesion, and odontogenic differentiation (with bio-chemicals).	downstream pathways.
Evaporation-induced self-assembly	MBG [140]	Fe:Ca=10:5	Facilitated osteoblast cell proliferation, ALP activity and osteogenic expression. However, it exhibited slightly slower apatite formation rate (with bio-chemicals).	Stabilized the pH value in the surrounding environment.
	MBG [141]	5%, 10% wt	Enhanced the mitochondrial activity and the expression of bone-related genes in hBMSCs attached to the scaffolds (no bio-chemicals).	Trace amounts of Fe^{3+} released from the scaffolds. And the beneficial pH environment.
	MBG [142]	Fe:Ca=10:5	Biocompatible, allowing cell attachment, proliferation, and differentiation	Not mentioned.
Solvent-casting techniques	PCL [143]	FeHA, 90/10, 80/20, 70/30, w/w	Favor cell viability and proliferation and support the osteogenic differentiation (with and without bio-chemicals).	The inclusion of FeHA nanoparticles intrinsically enhances the hydrophilicity and modifies the substrate topography.
LbL assembly	PLGA/PCL/gelatin [146]	16.4% wt	Significantly improved the hydrophilicity and stiffness of scaffold and enhanced the osteogenic differentiation of ADSCs.	The magnetism of nanoparticles was considered to play a critical role in improving osteogenesis.
Magnetic assist fabrication	α-Al_2O_3 [150]	STMF (≈ 25, 75, 150 mT)	Not detected.	Not detected.
	α-Al_2O_3 [151]	MF at 75 mT.	Not detected.	Not detected.
	PCL/gelatin [149]	10% wt	Mouse BMSCs attached within the scaffolds retained their osteogenic differentiation potential and deposited ECM (with bio-chemicals).	Combined the topographical features of nanofibers, magnetic assembly and multilayer 3D structure together to biomimic the ECM.

Abbreviations: MC: magnetic nanoparticles content; MI: magnetic intensity; HA: hydroxyapatite; Col: collagen; hBMSCs: human bone marrow stem cells; PVA: poly vinyl alcohol; MF-nHAp: multifunctional nano hydroxyapatite particles; PCL: poly(caprolactone); CPC: calcium phosphate cement; MBG: mesoporous bioglasses; STMF: static transverse magnetic field; MF: magnetic field; PLGA: poly(lactic-co-glycolic acid); FeHA: (Fe^{2+}/Fe^{3+})-doped hydroxyapatite; MNPs: magnetic nanoparticles; nFeHA: Fe doped nanohydroxyapatite; hDPCs: human dental pulp cells.

Table 3. Magnetic scaffolds with the application of magnetic fields for osteogenesis.

Magnetic scaffold	Magnetic field: Type and Intensity	Exposure method	Biological effects	Mechanisms
PCL/MNPs, 5% (1.7emu/g), 10% (4.8emu/g) w/w [157]	SMF, 15mT	Continuous exposure	The SMF synergized with the magnetic scaffold in enhance the osteoblastic differentiation of primary mouse calvarium osteoblasts (with bio-chemicals)	Activation of integrin signaling pathways, up-regulation of BMP2 and phosphorylation of Smad1/5/8, promote the angiogenic response of endothelial cells.
nHA/PLA/MNPs, 0.049 emu/g [156]	SMF, 0.05–0.2 mT (middle), 5–25 mT (two sides)	Continuous exposure	Accelerates new bone tissue formation and remodeling through synergizing with the applied static magnetic field in the rabbit defect.	The magnetic stimulation originated from the response of MNP embedded in the nanofibers to the external magnetic field.
nHA/PLA/ MNPs, 0.0492 emu/g [126]	SMF, 0.9–1.0 mT	Continuous exposure	Magnetic scaffold and SMF acted in a coordinated way to enhance the proliferation, differentiation and ECM secretion of the MC3T3-E1 cells (with bio-chemicals)	The interactions of the paramagnetic film and the static magnetic field with the cells.
PLA/ MNPs, 2.5, 5, w/w [127]	SMF, 100mT	Continuous exposure	The marriage of magnetic nanofibers and external SMF was found most effective in accelerating every aspect of biological behaviors of MC3T3-E1 osteoblasts (with bio-chemicals).	The iron ions released from MNPs. And the application of moderate-intensity SMF.
Co-nucleation of biomimetic HA and MNPs on collagen fibers [161]	SMF, 1.2T	Continuous exposure for 12 weeks	Bone defect in rabbit femoral condyle, the reorganization of the magnetized collagen fibers under the effect of the SMF produces a highly-peculiar bone pattern, with highly-interconnected trabeculae orthogonally oriented with respect to the magnetic field lines.	The transfer of micro-environmental information, mediated by collagen fibrils magnetized by MNPs, under the effect of SMF.

3D scaffold with collagen-chitosan -HA-MNPs coating [162]	SMF, 100- 250 mT	Continuous exposure	Synergic effect of 3D structure optimization and static magnetic stimulation enhances the osteogenic differentiation of MG-63 cells by 2 folds greater.	MNPs generate the microdeformation of the structure under SMF, providing strain stimulation to the seeded cells.
FeHA/collagen, 70/30 wt % [163]	SMF, 320 mT	Continuous exposure	The magnetization of the super-paramagnetic scaffolds, induced applying an external SMF, improved MG63 cell proliferation (with bio-chemicals).	Not mentioned.
PCL/FeHA, 80/20 w/w [132]	SMF	24h since cell seeding	Under SMF, the loading of magnetic labeled BMSCs into the scaffolds was 36% higher. Cell growth after magnetically assisted loading was 2.2-fold greater.	When the scaffolds were loaded in the presence of a magnetic field, the cell attachment was more consistent amongst replicates.
nHA/PLLA/ MNPs [164]	PEMF, 100mT	Not mentioned	Magnetic scaffold combined with PEMF enhanced the osteogenic differentiation of Rabbit BMSCs	MNPs have the ability to bind to the cell surface, and can control and regulate the function of the cells under the applied PEMF.

Abbreviations: PCL: poly(caprolactone); MNPs: magnetic nanoparticles; BMP2: bone morphogenetic protein-2; nHA: nano hydroxyapatite particles; HA: hydroxyapatite; PLA: polylactic acid; SMF: static magnetic field; PEMF: pulsed electromagnetic fields.

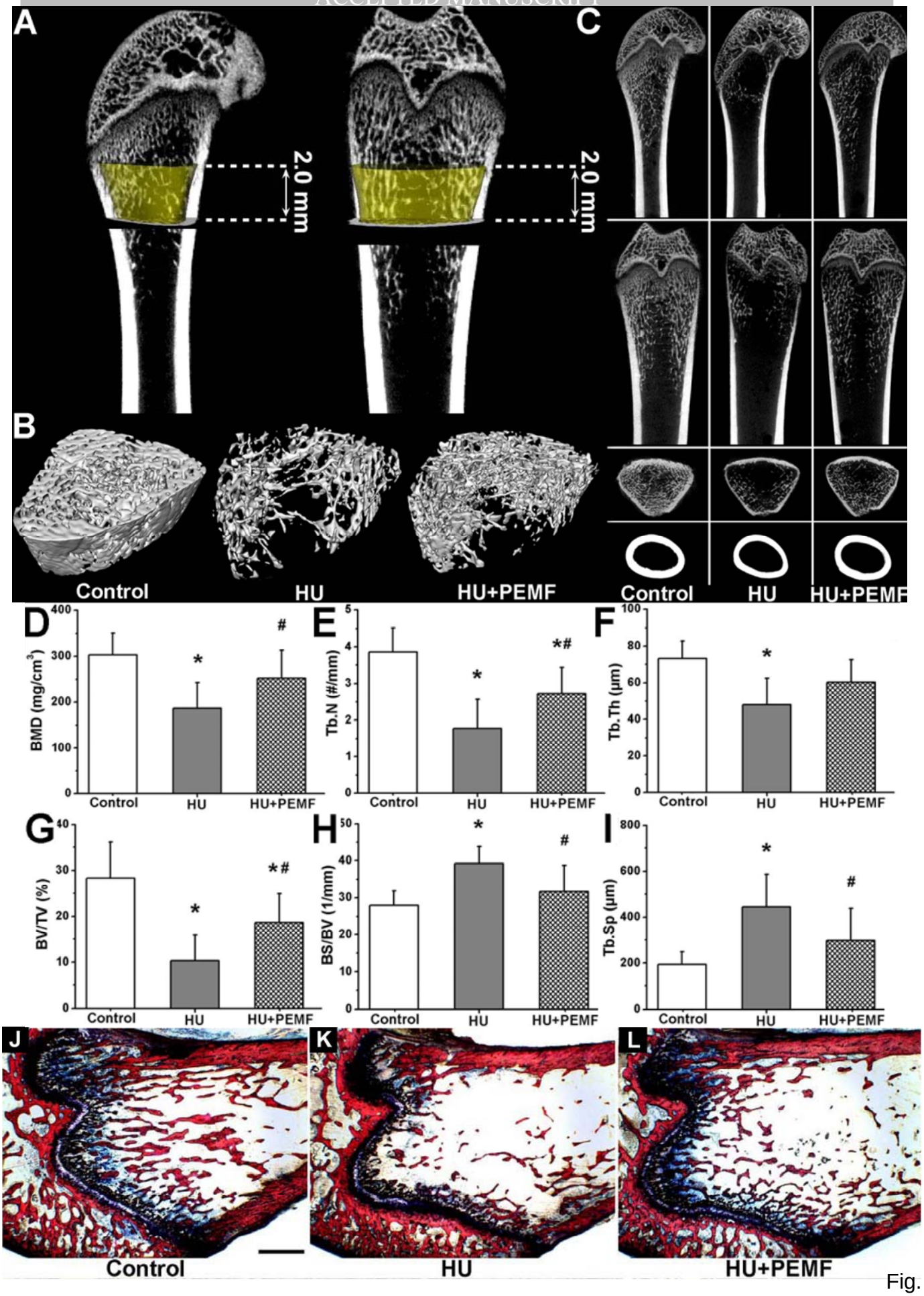

Fig. 1

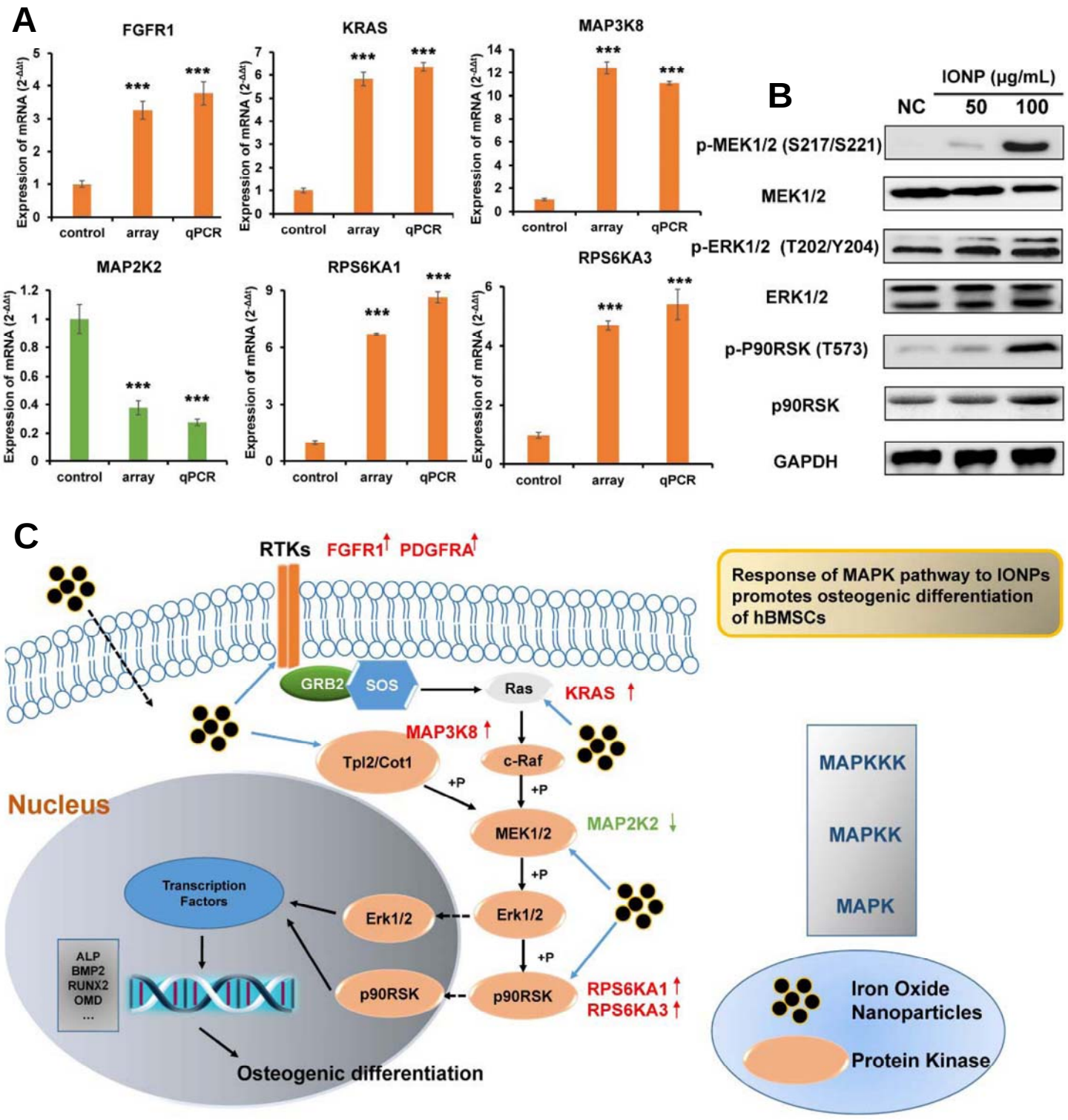
A
FGFR1
KRAS
MAP3K8
MAP2K2
RPS6KA1
RPS6KA3
Expression of mRNA (2-ΔΔt)
control
array
qPCR
***
B
IONP (μg/mL)
NC
50
100
p-MEK1/2 (S217/S221)
MEK1/2
p-ERK1/2 (T202/Y204)
ERK1/2
p-P90RSK (T573)
p90RSK
GAPDH
C
RTKs
FGFR1
PDGFRA
GRB2
SOS
Ras
KRAS
MAP3K8
Tpl2/Cot1
c-Raf
+P
MEK1/2
MAP2K2
Nucleus
Transcription Factors
Erk1/2
p90RSK
RPS6KA1
RPS6KA3
ALP
BMP2
RUNX2
OMD
...
Osteogenic differentiation
Response of MAPK pathway to IONPs promotes osteogenic differentiation of hBMSCs
MAPKKK
MAPKK
MAPK
Iron Oxide Nanoparticles
Protein Kinase

Fig. 2

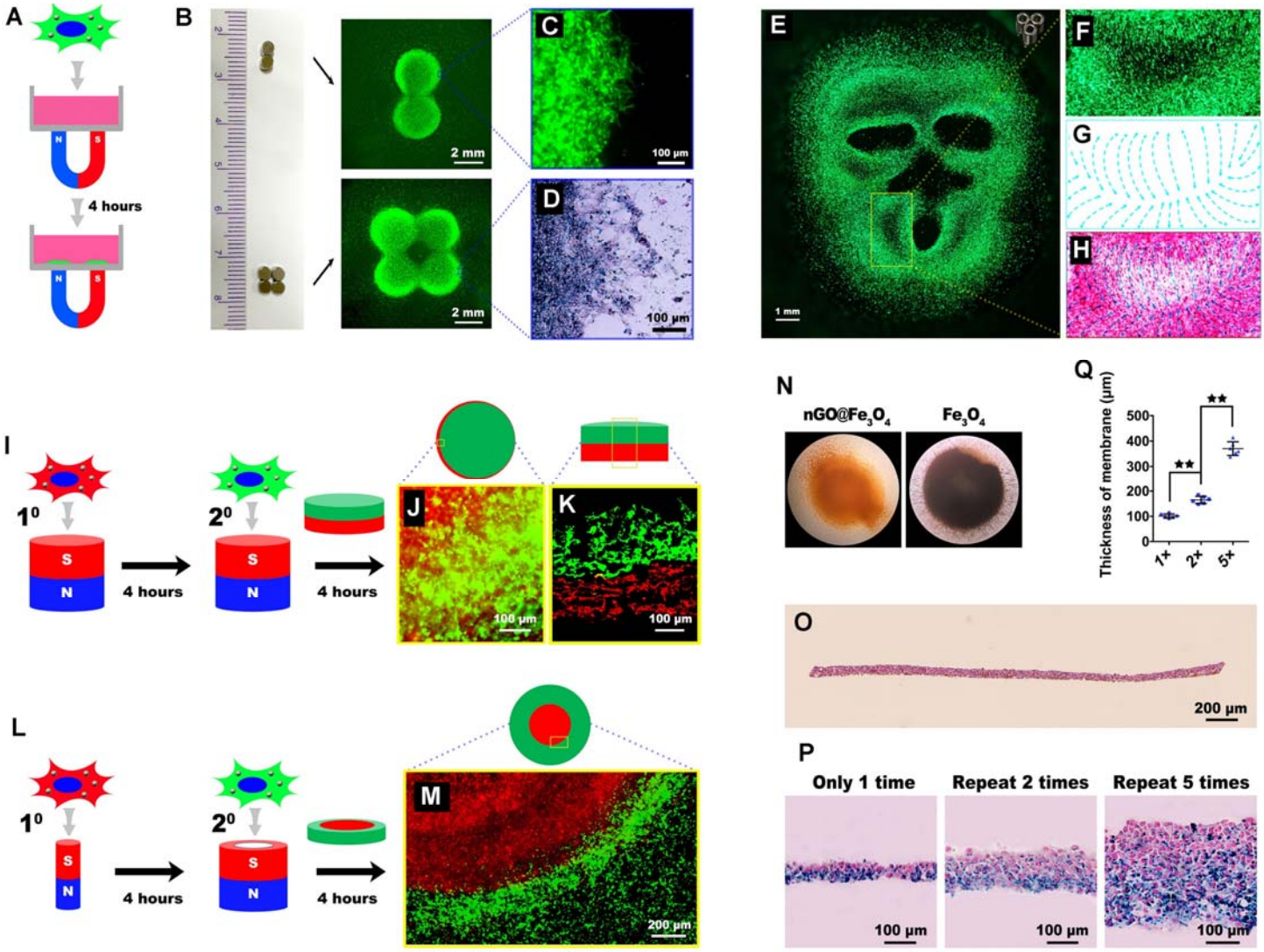
A
4 hours
B
C
2 mm
100 μm
D
2 mm
100 μm
E
1 mm
F
G
H
I
1⁰
4 hours
2⁰
4 hours
J
100 μm
K
100 μm
L
1⁰
4 hours
2⁰
4 hours
M
200 μm
N
nGO@Fe3O4
Fe3O4
Q
Thickness of membrane (μm)
500
400
300
200
100
0
1+
2+
5+
O
200 μm
P
Only 1 time
Repeat 2 times
Repeat 5 times
100 μm
100 μm
100 μm

Fig. 3

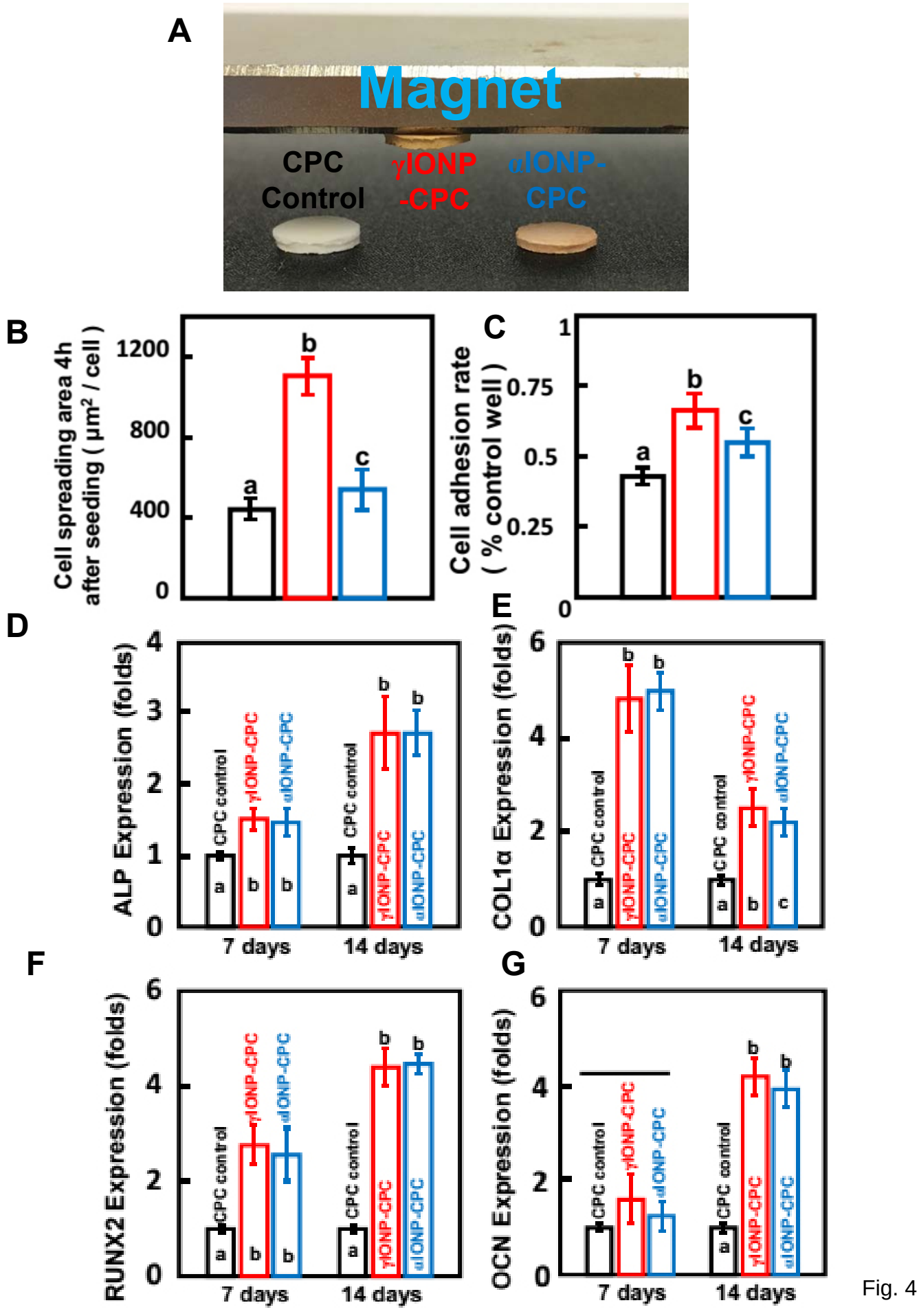
A
Magnet
CPC Control
γIONP -CPC
αIONP-CPC
B
Cell spreading area 4h after seeding (μm² / cell)
1200
800
400
0
a
b
c
C
Cell adhesion rate (% control well)
1
0.75
0.5
0.25
0
a
b
c
D
ALP Expression (folds)
4
3
2
1
0
CPC control
γIONP-CPC
αIONP-CPC
7 days
14 days
E
COL1α Expression (folds)
6
4
2
0
F
RUNX2 Expression (folds)
G
OCN Expression (folds)

Fig. 4

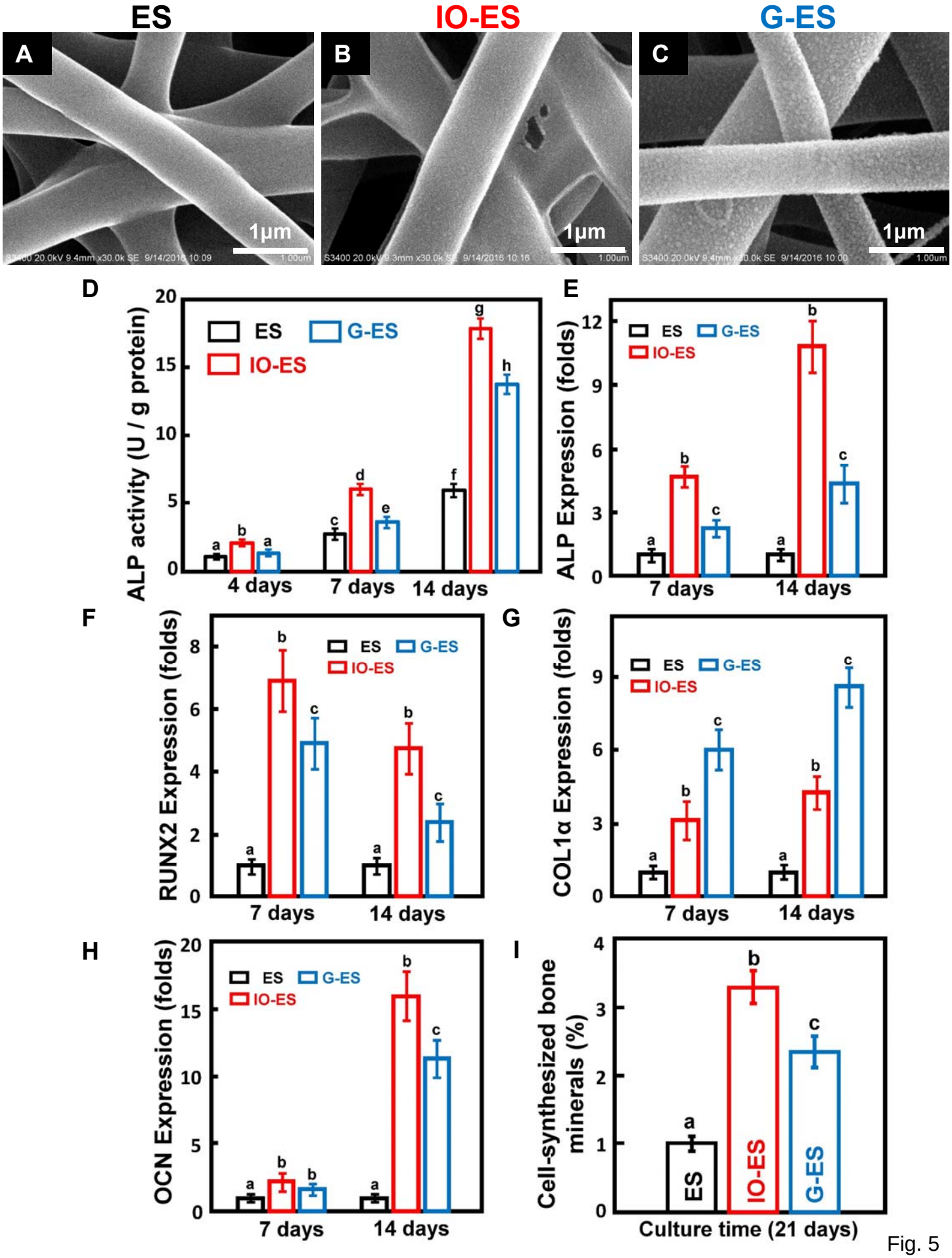

Fig. 5

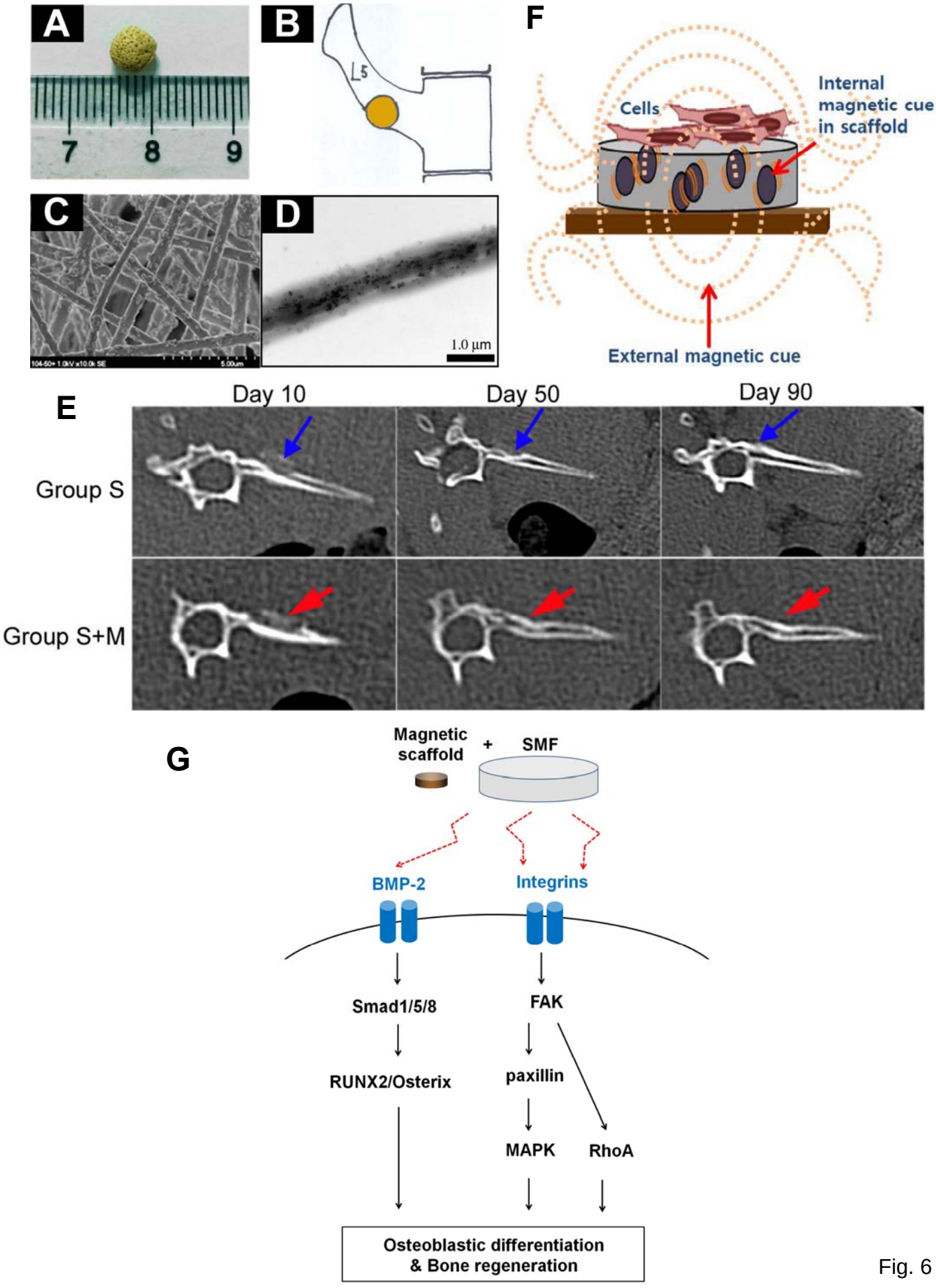
A
B
L5
C
D
1.0 μm
F
Cells
Internal magnetic cue in scaffold
External magnetic cue
E
Day 10
Day 50
Day 90
Group S
Group S+M
G
Magnetic scaffold
+
SMF
BMP-2
Integrins
Smad1/5/8
FAK
RUNX2/Osterix
paxillin
MAPK
RhoA
Osteoblastic differentiation & Bone regeneration

Fig. 6

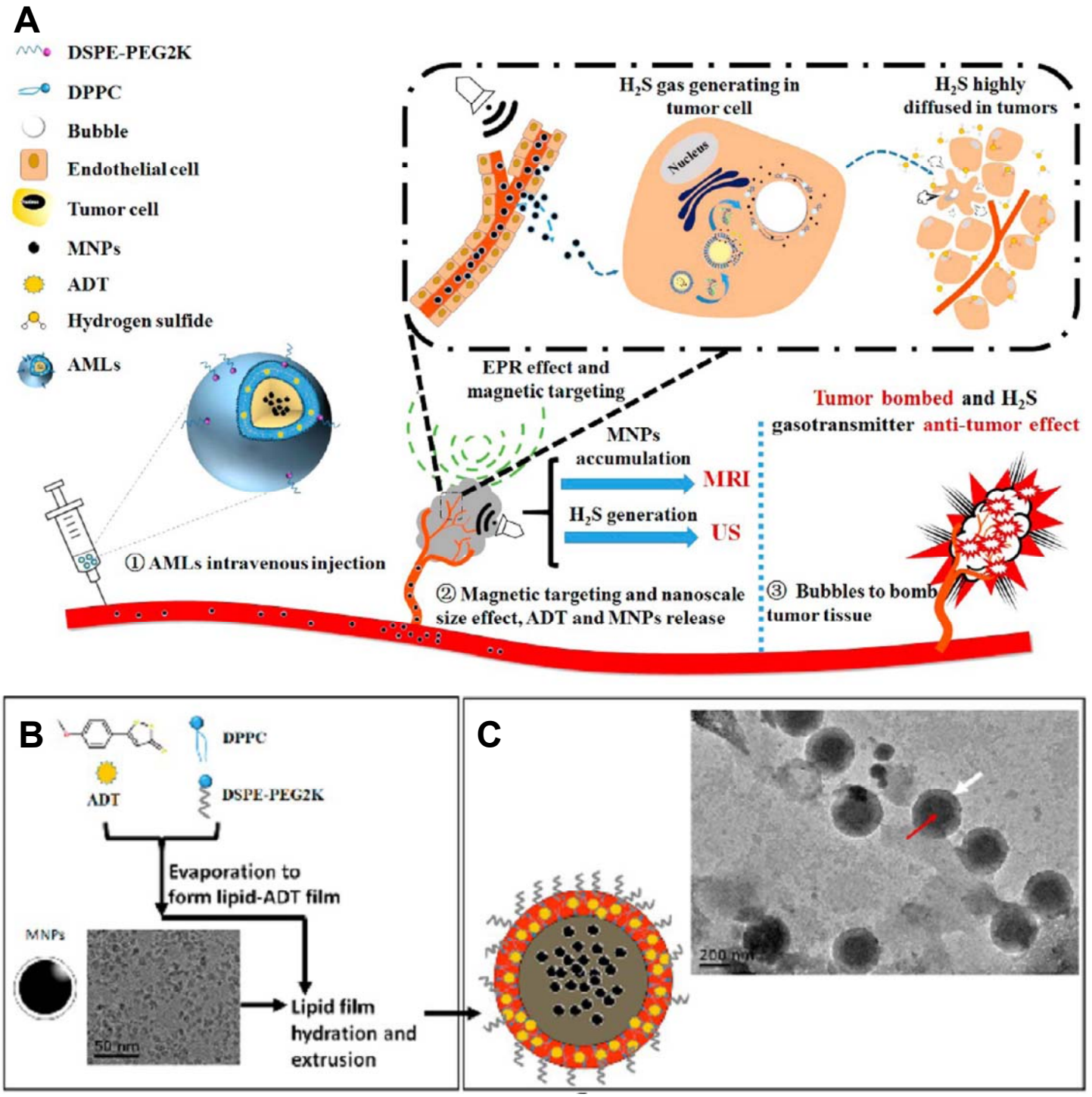
A
DSPE-PEG2K
DPPC
Bubble
Endothelial cell
Tumor cell
MNPs
ADT
Hydrogen sulfide
AMLs
H2S gas generating in tumor cell
H2S highly diffused in tumors
Nucleus
EPR effect and magnetic targeting
Tumor bombed and H2S gasotransmitter anti-tumor effect
MNPs accumulation
MRI
H2S generation
US
① AMLs intravenous injection
② Magnetic targeting and nanoscale size effect, ADT and MNPs release
③ Bubbles to bomb tumor tissue
B
DPPC
ADT
DSPE-PEG2K
Evaporation to form lipid-ADT film
MNPs
50 nm
Lipid film hydration and extrusion
C
200 nm

Fig. 7

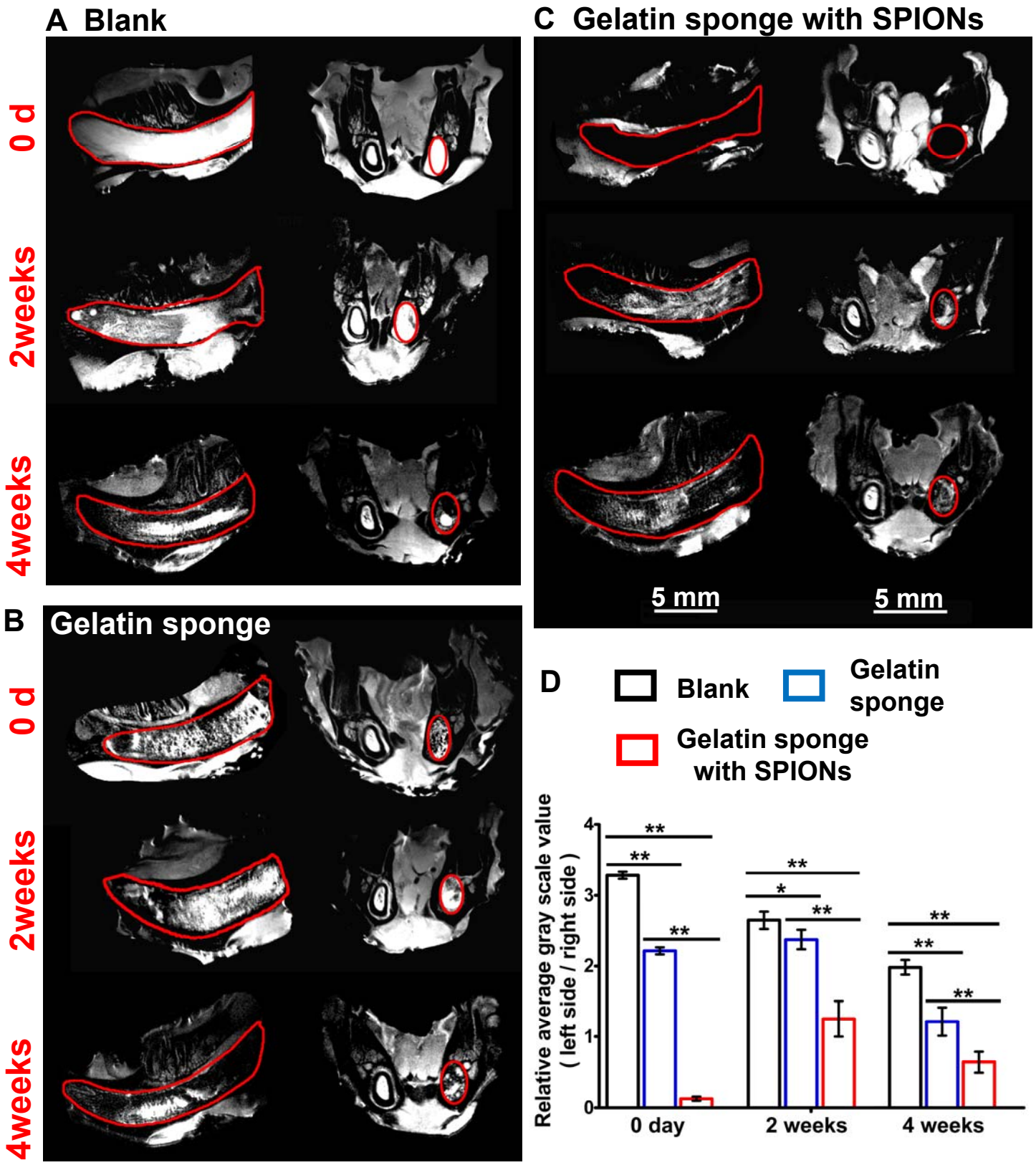
A Blank
C Gelatin sponge with SPIONs
0 d
2weeks
4weeks
B
Gelatin sponge
0 d
2weeks
4weeks
5 mm
5 mm
D
Blank
Gelatin sponge
Gelatin sponge with SPIONs
Relative average gray scale value (left side / right side)
0 day
2 weeks
4 weeks

Fig. 8